Recent advances in hard-magnetic soft composites: Synthesis, characterisation, computational modelling, and applications

Sergio Lucarini, Mokarram Hossain, Daniel Garcia-Gonzalez

PII: S0263-8223(21)01246-0
DOI: https://doi.org/10.1016/j.compstruct.2021.114800
Reference: COST 114800

To appear in: *Composite Structures*

Received date : 1 June 2021
Accepted date : 6 October 2021

Please cite this article as: S. Lucarini, M. Hossain and D. Garcia-Gonzalez, Recent advances in hard-magnetic soft composites: Synthesis, characterisation, computational modelling, and applications. *Composite Structures* (2021), doi: https://doi.org/10.1016/j.compstruct.2021.114800.

Recent advances in hard-magnetic soft composites: synthesis, characterisation, computational modelling, and applications

Sergio Lucarini[a], Mokarram Hossain[b,*], Daniel Garcia-Gonzalez[a,*]

[a]Department of Continuum Mechanics and Structural Analysis, Universidad Carlos III de Madrid, Avda. de la Universidad 30, 28911 Leganés, Madrid, Spain
[b]Zienkiewicz Centre for Computational Engineering, College of Engineering, Swansea University, SA1 8EN, United Kingdom

---

Abstract

Hard-magnetic soft composites consist of magneto-active polymers (MAPs) where the fillers are composed of hard-magnetic (magnetically polarised) particles. These novel multifunctional materials are experiencing a great advance from the last few years. This rise has been motivated by the possibility of controlling ferromagnetic patterns during the manufacturing process. Thus, structures with programmable functionalities can be conceptualised and implemented, opening new routes into the design of smart components with great opportunities in the biomedical engineering and soft robotics fields. In this work, we provide an overview of the state of the art of such MAPs, providing the key fundamentals and reference works. To this end, we present the current synthesis and experimental characterisation methods, the different computational modelling approaches across scales, and a detailed presentation of their current potential applications. Finally, we provide an overall discussion on future perspectives.

Keywords: Magneto-active polymers (MAP), Hard-magnetics, Magneto-mechanics, Smart materials, Constitutive modelling, Multifunctional composites

---

1. Introduction

When designing structural components, the choice of the materials to be used in their manufacturing has traditionally been made by taking considerations based on mechanical properties such as stiffness, maximum strength or density. Recently, this choice has experienced a paradigm shift with the possibility of including, during the designing process, not only structural characteristics but also other functionalities. These new possibilities have arisen from the development of novel multifunctional smart materials. The multifunctionality of a material is understood as its capacity to present alterations in its mechanical properties or deformation with the application of an external physical stimulus; or vice-versa, the alteration of a given functionality with the application of mechanical loading. Among these multifunctional, also called smart materials, we find electro- [1, 2] and magneto-active [3, 4, 5], thermo- [6, 7] and photo-responsive [8], pH- and chemo-sensitive composites [9]. All these alternatives have provided new routes into the design of smart systems that can be mechanically-responsive to external stimuli. However, most of them present certain limitations to control their response remotely. For example, photo-responsive materials are limited by the opacity of the surrounding media, electro-active materials usually need a direct contact with the

---

*Corresponding authors
Email addresses: `slucarin@ing.uc3m.es` (Sergio Lucarini), `mokarram.hossain@swansea.ac.uk` (Mokarram Hossain), `danigarc@ing.uc3m.es` (Daniel Garcia-Gonzalez)

stimulation system, and others such as thermo- or pH-responsive materials sometimes require restricted environmental conditions. In this regard, magneto-active materials can overcome many such limitations if the presence of ferromagnetic domains can be avoided, which make them ideal candidates for many applications within the biomedical field, thanks to the low magnetic permeability of the biological tissues. In addition, a good interphase with biological tissues can be reached by developing soft magneto-active systems by using polymeric materials such as elastomers and hydrogels [10]. These characteristics also make magneto-active materials as excellent candidates for other applications such as in soft robotics, tetherless actuations or soft sensor-actuator systems [11, 12].

Magneto-active polymers (MAP) are a class of smart materials that mechanically respond to external magnetic stimuli. Ideally, these composites consist of a polymeric matrix filled with magnetisable particles. Such a matrix could be either a soft elastomer or an extremely soft hydrogel or a shape memory polymer, for different soft matrix materials, see [22, 23]. Under the application of an external magnetic field, the particles interact among themself and with the externally applied magnetic field. Such interactions result into internal forces and torques that make the particles to attract or repulse each other and rotate, respectively. However, the magnetic particles are not isolated but intrinsically linked by the polymeric matrix that acts as a continuum medium transmitting the generated forces within the particles. Therefore, the response of MAPs as a system strongly depends on the nature of both polymeric matrix and the magnetic particles as well as their bondings. Depending on the polymer used for the matrix, different stiffness can be achieved ranging from very soft hydrogels to relatively stiff thermoplastic polymers [13, 14]. The stiffness of the matrix thus determines the magnetorheological response of MAPs, i.e., the softer the matrix, the higher mechanical deformation experienced by a MAP as a result of the externally applied magnetic field.

A common solution widely proposed in the literature is the use of elastomeric matrices [15], that have stiffnesses between hydrogels and thermoplastics. Regarding the nature of the active particles, these can be grouped into two main classes: soft-magnetic [15] and hard-magnetic [4]. Soft-magnetic particles (e.g., iron particles) present a low magnetic coercivity. Under a null external magnetic field, these particles have a null magnetisation. When a magnetic field is applied, MAPs' magnetisation evolves leading to dipole-dipole interactions introducing some internal stresses within the composites which further induce deformations or changes into its mechanical properties [16]. On the contrary, hard-magnetic particles can sustain a given magnetisation even under a null external magnetic field after the removal of an applied applied field. As a consequence, upon further application of an external magnetic field, these particles trend to align in the field direction introducing internal torques within a MAP [17]. Such an effect allows for programming specific mechanical responses, in a shape-transformation fashion, to different magnetic stimulation [18].

Due to their specific nature and magneto-mechanical couplings, soft- and hard-magnetic polymers can be found in many promising applications. Overall, soft-magnetic MAPs outstand for applications that require large reversible volume or areal deformations. Among them, we can find applications such as precision and controlled drug delivery, microfluidic valves, water purification treatment or soft robotics [19, 20]. Hard-magnetic MAPs (here we call them hMAPs), instead, present great opportunities for applications that require fast shape changes. Some of the most interesting applications of these materials are in soft robotics [11, 12], shape morphing and flexible structures [4], and biomedical devices [3], to mention a few. Moreover, the design and conceptualisations of these smart systems are highly complex as one must account at the same time for materials science, mechanics, and magnetics fundamentals (among others). To help at this complex endeavour, advances in the manufacturing techniques and modelling approaches provide new routes to overcome limitations and go beyond the current bottlenecks. In this regard, novel manufacturing techniques have recently been developed, such as the 3D printing of ferromagnetic domains controlling the magnetisation of the particles [4], or a new approach to re-configure these magnetisation patterns [109]. Modelling approaches have also experienced great advances with new approaches to simulate the magneto-mechanical response of MAPs [17, 21].

In this article, we focus on hMAPs and present an overview of their current state of the art. It also provides the main fundamentals and reference works to get into the topic. To this end, we have structured the content covering all the relevant perspectives. First, the synthesis methods for hMAPs are presented along with the experimental characterisation techniques to date. Secondly, the computational modelling procedures of hMAPs are introduced collecting the most important theoretical bases and different numerical approaches across the length. scales. A detailed presentation of their current applications is then presented. Finally, we provide a final discussion on the future perspectives.

2. Synthesis and experimental characterizations

2.1. Synthesis of hard-magnetic soft composites

Manufacturing processes have significant influences on the functionalities and intricate designs of the hMAPs. The techniques for synthesising magneto-active soft polymeric composites can be divided into two major groups: i) traditional methods, and ii) additive manufacturing (AM) or 3D printing methods. Moreover, some efforts have been seen in the literature where researchers try to combine traditional manufacturing techniques along with advanced 3D printing methods, e.g., see for instance, Lee et al. [160].

2.1.1. Traditional synthesis methods

Moulding is one of the most widely used classical manufacturing processes for any polymeric composites. The process, being suitable both for hMAPs and soft-magnetic composites, is relatively easy for scale up. In preparing magnetic composites, soft polymeric matrix is mixed up with magnetic fillers and let them to cure. In order to manufacture hard- or soft-magnetic composites with enhanced actuation properties, a magnetic field can be applied during the solidification (curing) process resulting in chain-like anisotropic microstructures. Moreover, in order to create intricate magnetic programming within a MAP, distributed and well-structured magnetisations need to be induced in the structure. These types of well-designed spatially-varied composites will be capable of creating complex and desired magnetic shape-morphing structures, particularly used in soft robotics. However, such well-designed magnetisation is difficult to produce using classical manufacturing techniques such as the moulding. Sometimes, it is possible to create spatially distributed magnetisations in hMAPs if only a massive amount of magnetic field is applied in a fully solidified magnetic composite containing hard-magnetic particles. For example, Lum et al. [18] successfully used the traditional moulding technique to produce shape-morphing structures made of hMAPs in which elastomer is used as the matrix, while Hu et al. [161] also used the moulding technique to synthesise hydrogel-based hard-magnetic anisotropic soft materials. Moreover, using a traditional moulding technique, Alfadhel and Kosel [96] synthesised magnetic cilia tactile sensors that contain hard-magnetic nano particles. For a comprehensive route for manufacturing hMAPs-based structures using the moulding technique, see Figure 1.

2.1.2. Additive manufacturing or 3D printing methods

The ASTM (American Society for Testing and Materials) International Committee F42 on the Additive Manufacturing (2009) divided all 3D printing techniques of soft polymeric materials into seven main categories [24]. Among them, Material Extrusion, Material Jetting, and Vat Photopolymerisation are most

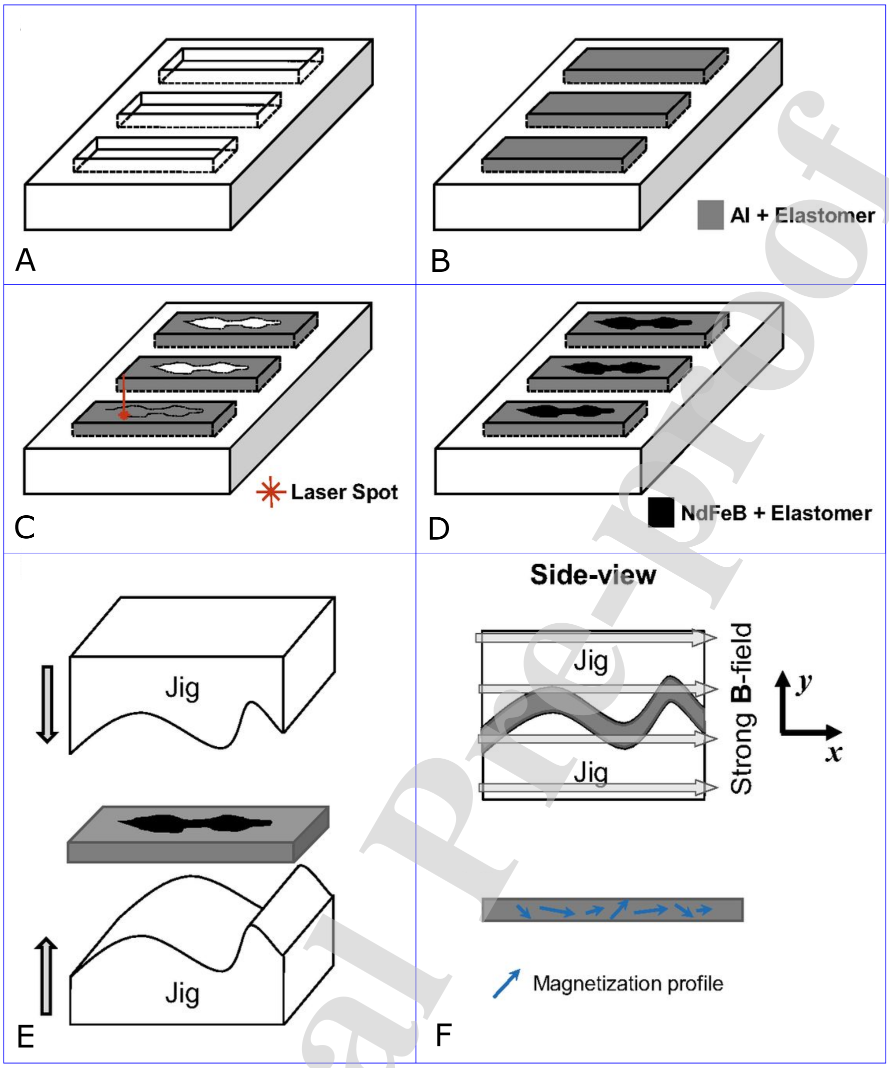

Figure 1. The fabrication of a beam-like structure made of hMAPs using the classical moulding technique: (A) a negative mould for the beam; (B) the passive component containing aluminum (Al) powder and Ecoflex silicone elastomer that was poured into the mould in liquid form and allowed to cure; (C) a laser cutter is used to create a band of nonuniform width containing the continuum magnitude profile of magnetisation; (D) the active component of a hard-magnetic filler (NdFeB) with a silicone (Ecoflex) matrix which was then poured and cured to replace the band; (E) the beam was bent into the jig profile; (F): (above) the beam was magnetized with a strong $\mathbb{b}$ field (1 T); (below) the desired magnetisation profile is created after removing the beam from the jig (Figure taken from Lum et al. [18]).

widely used in the 3D printing of magneto-active composites, irrespective of hard- or soft-magnetic fillers. Note that these printing techniques are further grouped into several subsets. In the following sections, we will briefly discuss three main printing methods along with a few of their variations that are widely used in the 3D printing of hMAPs.

Material Jetting-based printing

Material Jetting is a well established 3D printing process that works by obtaining slicing data from the computer aided design (CAD) inputs and a photo-curable ink that is selectively deposited based on the object representation on a substrate via ink droplets. The ink can be deposited either using a continuous jetting system or a drop-on-demand (DOD) system. In the case of continuous jetting process, inks are seamlessly streamed out from the nozzle (also known as the print head) under pressure. At the same time, the jetting ink is broken into charged droplets as a result of an electric field. In contrast, in the case of DOD system, a thermo or piezoelectric actuator creates pulses that help in ejecting a single ink droplet from an ink volume when required. Note that these photo-curable inks can be composed of monomers, macromers (known as oligomers), photoinitiators, additives, curatives, colourants (for making colourful objects) etc. Hence, it is relatively easy to add magneto-active fillers in the inks prior to the printing process using a Material Jetting process. Since, in this technique, inks can be deposited when required, multiple print heads can be used at a time. Once ink droplets are deposited, they are cured with an UV light, see Wang et al. [25] for a detailed review on the Material Jetting-based printing techniques. For instance, very recently, Sundaram et al. [162] developed a bespoke MJ-based printing system that enables the rapid fabrication of multi-material structures in which nano-size soft-magnetic particles are used. However, the same technique can easily be adopted to nano-size hard-magnetic fillers. For a schematic of the Material Jetting process, see Figure 2A.

Material Extrusion-based printing

In Material Extrusion AM method, inks are polymeric solutions, pastes, molten and semi-molten polymers, dispersions etc which are extruded through a tiny orifice or nozzle known as the print head. This 3D printing technique can be classified into two main categories, i.e., Fused Deposition Modeling (FDM) and Direct Ink Writing (DIW). First one is the FDM in which a thermoplastic polymer feed as the filament form is melted with sufficient heat in the extruder before it is deposited layer-by-layer on the build platform as per the computer program. In FDM, several print heads can be used to deposit few polymers of different mechanical and chemical properties simultaneously. Such a feature gives ample of opportunities in printing spatial-varying mechanical properties. Furthermore, one of the print heads can be used to deposit support materials for 3D printed complex structures. The building chamber is usually preheated to reduce thermal distortion that may arise during a non-uniform cooling. However, the intimate blend of colours achieved in the FDM technique is not as high quality as that achieved in the MultiJet printer. In some senses, FDM is an updated version of the conventional extrusion or injection moulding except that the technique does not require any mould to provide the part with the expected shape. A schematic of the Material Extrusion-based (e.g., FDM) is presented in Figure 2B. Note that FDM and SLS (selective laser sintering) are similar in the aspect that both use polymer preform as the initial materials, see Rafiee et al. [26], Li et al. [30], Ligon et al. [24], Tareq et al. [34] for more details. For instance, Kim et al. [4] used a DIW technique, a major sub-set of the Extrusion-based 3D printing technique, for the 3D printing of ferromagnetic domains.

Vat-based Photopolymerization printing

Vat Photopolymerization is one of the oldest additive manufacturing processes for polymers in which a light-cured liquid photoresin (uncured polymer) containing in a vat (hence, the name Vat Photopolymerisation) is selectively cured by a light source. Depending on the type of light source and scanning process of the light, Vat Polymerisation has several variants such as SLA (stereolithography), DLP/DLS (digital light processing/digital light synthesis), 2PP (two photon photopolymerisation), Rapid Liquid Printing, Volumetric 3D Printing, micro-lithography etc. In SLA, an UV laser or an UV LED (light-emitting diode) source induces light on a particular point in the x-y plane representing an object directly from the CAD geometry. Once a point is irradiated through the UV laser source, it moves to the next point (hence it is called a point-by-point photocuring process) on the x-y plane and continues until one layer is irradiated. Afterwards, the light

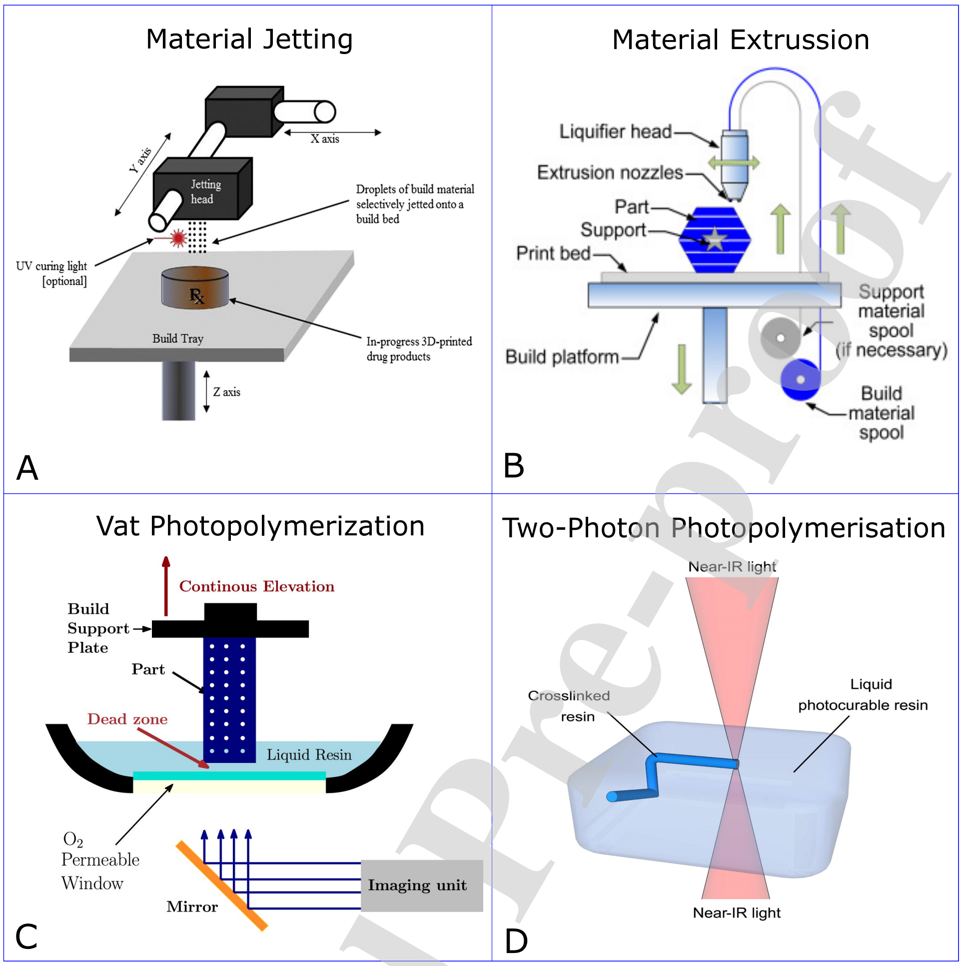

Figure 2. Four major additive manufacturing (AM) methods widely used in printing hard-magnetic soft composites: A) A Material Jetting-based printing method (Figure is reproduced from Norman et al. [29]), B) A Material Extrusion-based printing such as the FDM method (Figure taken from Ning et al. [28]), C) A Vat-based printing technique such as the Digital Light Projection/DLP (Photo courtesy from Hossain et al. [32]), D) A schematic diagram of the Two-Photon Photopolymerisation (i.e., 2PP) printing technique that is well-known in the manufacturing of micro-to nano-scale hard-magnetic composites (Figure taken from Billiet et al. [27]).

source moves up or down (depending on the movement of the support platform) in the z-axis. In contrast to the SLA, DLP has several advanced features. First, instead of the point-by-point curing, the light source cures an entire layer at once. In addition, DLP uses a UV light by a projection instead of a laser. One of the most salient features of the DLP is that it is much faster that the traditional SLA. Moreover, DLP is less influenced by the oxygen inhibition as it has oxygen permeable Teflon layer at the bottom, see Figure 2C. When oxygen permeates through the window, it creates an extremely thin layer (similar to a human hair) between the resin and the permeable window which is called the dead zone of uncured resin. This oxygen inhibit zone restrict photocuring of the bottom layer adjacent to the window and helps in keep flowing the liquid resin continuously. Therefore, it is a continuous 3D printing process rather than a layer-by-layer or a dot-by-dot printing process. One of the advanced DLP methods (initially known as the Continuous Liquid Interface Production, CLIP) is due to Carbon3D devised by DeSimone and co-workers [31]. The key features of the DLP printing technique are sketched in Figure 2C.

Very recently, Xu et al. [85] developed a method for patterning hard-magnetic microparticles in an elastomer matrix using a DLP-based 3D printing, while Nagarajan et al. [163] explored a wide range of DLP-based 3D printing techniques for both soft- and hard-magnetic fillers. Although Lantean et al. [164] and Domingo-Roca et al. [33] used the DLP-based 3D printing for soft-magnetic composites only, this can also be adopted for hard-magnetic fillers as they used nano-size particles in order to avoid particle sedimentation. One of the most favoured Vat-based 3D printing techniques for micron-scale fabrications is the so-called multi-photon polymerisation (also known as two-photon polymerisation or direct laser writing). In two-photon (i.e., 2PP) process, laser pulses at 800 nm wavelength is focused on photo-polymerisable resins containing in a vat to initiate the curing process. Once laser beam focuses a small volume of photoresin in which a suitable photoinitiator will absorb the two photons of 800 nm wavelength and act as a one photon of 400 nm wavelength which is the range of UV light region. Such a photoinitiator will help in initiating cross-linking reactions among initiators, monomers and cross-linkers. In 2PP, the laser only focuses a tiny volume of photo-sensitive resin for creating a 3D printed object without affecting areas outside the focal point. Such an excellent characteristics of creating micron to nanoscale fabrications, 2PP becomes one of the most used techniques in micro-and nanoscale soft robots using soft and hard-magnetic polymeric composites. A rough sketch of the 2PP printing method is depicted in Figure 2D.

2.2. Experimental characterisation of hard-magnetic soft composites

Magneto-active polymers as soft materials may undergo various forms of deformation with and without an externally applied magnetic field during their service life. A magnetic field creates broadly two types of effects on MAPs. First, it changes their rheological properties such as storage and loss moduli, frequency, relaxation behaviour, damping properties etc., see Bastola et al. [36]. Second, it induces shape-morphing capabilities that result in various forms of deformations, e.g. tension, compression, shear etc. Moreover, due to the programmable patterns resulting from the magnetic particles (especially hard-magnetic particles), spatially-varying magnetic domains can be created in hMAPs that are mainly responsible for the shape-morphing behaviour. Thus, hMAPs can create various shape-shifting capabilities such as jumping, crawling, bending, twisting etc. Note that not only programmable properties are responsible for the shape-changing, time and space-varying magnetic fields are also necessary, see Wu et al. [68]. In order to quantify the influences of a magnetic field at small-strains, magneto-rheological experiments need to be conducted. For that, the rheometer test is a classical way to identify MAPs' rheological properties with and without a magnetic field, see Bastola et al. [36], Bastola and Hossain [37].

In contrast to the rheometer tests suitable for small-strain cases, as hMAPs are largely deformable, we need to perform experiments at finite strains. These include tension, compression, and shear tests, mostly suitable for soft MAPs. Moreover, loading-unloading cyclic, single- and multi-step relaxation tests at large deformations are required both for soft and hard magnetic composites. For instance, in order to understand the dissipative behaviour of MAPs at various fractions of fillers, several classes of mechanical tests such as loading-unloading cyclic tests at different strain rates, simple and multi-step relaxation tests are essential. At first, these tests under a purely mechanical load will quantify the influences of filler fractions. Furthermore, similar tests can be performed under a magneto-mechanically coupled field so that the change of various quantities such as stiffness, relaxation, magnetisation with respect to the magnetic field can be identified, see Stepanov et al. [155]. For instance, under a magnetic field, viscoelastic dissipative behaviour quantified

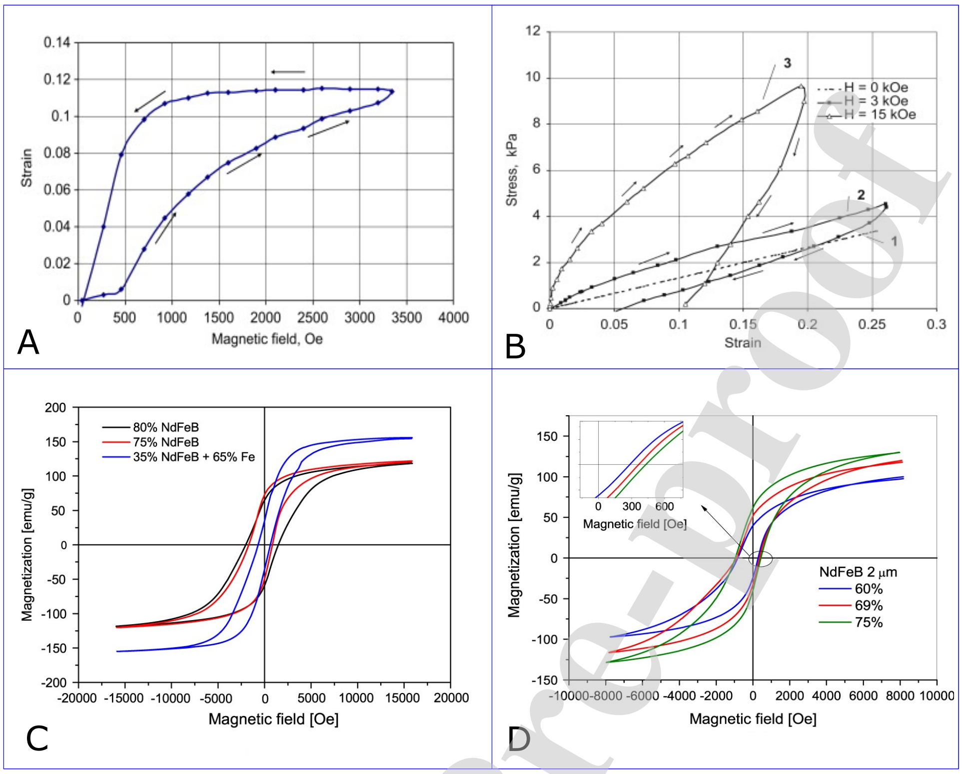

Figure 3. Magneto-mechanical experiments on hMAPs: A) Magnetostriction phenomenon is illustrated by the deformation of a sample under the influence of an external magnetic field in which arrows show the way of magnetic field change; B) Stress–strain curves demonstrating the effects of magnetization in hMAPs under the magnetic field of 3 kOe (2) and 15 kOe (3) in which an increasing magnetic field results in a larger hysteresis loop with a greater residual strain. Figures A and B are taken from Stepanov et al. [155]. C-D) the effects of hard-magnetic and soft-magnetic particles on the magnetic hystereses (Figures C & D are taken from Kramarenko et al. [157]).

by the loading-unloading cyclic tests will be enhanced. Note that constitutive modelling and simulation of hMAPs are active fields of current research. In contrast to experimental works on soft-magnetic composites, laboratory works demonstrating various key features of hMAPs are scare in the literature.

One of the earliest viscoelastic studies of hard-magnetic composites at finite strains is due to Stepanov and co-workers, e.g., [155, 157]. Therein, authors studied the viscoelastic and deformation behaviour of a hMAP-filled silicone elastomer under the influence of a magnetic filed, see Figure 3A. They observed that, in contrast to the soft-magnetic composites, hard-magnetic particles induce non-recoverable residual strains even in the absence of a magnetic field. These residual strains will increase with the increase of the applied field, see Figure 3B. Moreover, their study demonstrated that the elastic modulus of composites is strain-dependent in which an external magnetic field enhances the storage modulus and reduces the loss modulus significantly. More experimental data on hMAPs can be obtained in Antonel et al. [156], Kramarenko et al. [157], Koo et al. [158], Lee et al. [159]. A summary of Stepanov's seminal experimental works is depicted in Figure 3. These types of experiments at large strains produce sufficient data to feed the modelling frameworks described in the section below. In addition to the aforementioned viscoelastic tests, fatigue tests are also required to understand the life cycle of MAPs particularly in the application areas of shock and vibration, in which repeated cyclic loading is a common phenomenon, see Bastola and Hossain [35] for a comprehensive review on the experimental characterisation of magneto-active elastomeric composites.

3. Computational modelling of hard-magnetic soft composites

This section presents some basics for the constitutive modelling of hard-magnetic soft composites (hMAPs). First, we introduce the physical processes involved in the magneto-mechanical response of MAPs highlighting the main differences between soft- and hard-magnetics, from both macro- and micro-scale perspectives. Then, the key fundamentals of magneto-mechanics at finite strains are presented. Finally, these mathematical formulations are taken to further introducing the most relevant approaches in the literature based on macrostructural and microstructural bases.

3.1. The physics of hard-magnetic soft composites

A hMAP can be understood as the combination of two different phases that are connected each other presenting an intrinsic magneto-mechanical coupling at the microstructural level that determines its macrostructural responses. From a microstructural point of view, the hMAP consists of hard-magnetic particles that are distributed within a soft polymeric matrix. These magnetic particles have a high remanence magnetisation (or a residual magnetic flux). Such a strong magnetic remanence presents a given magnitude and orientation. Therefore, under the application of an external magnetic field, these particles trend to align along the magnetic field direction. As the particles are joined to the polymeric networks, this reorientation is not free but opposed by the mechanical resistance of the polymeric chains to reorient and deform. This mechanical interaction generates a series of micro-torques (hence macro-torques) within the composite as shown in Figure 4. When scaling up these micromechanics to the macro-scale, an effective macroscopic torque is observed acting on the composite and leading to significant mechanical deformations by means of both material rotation and stretch (represented by the total deformation gradient $\boldsymbol{F}$, will be discussed in the following sections), see Figure 4. These features make hMAPs as one of the most ideal candidates for manufacturing structural components with programmed changes in shape, controlling mechanical responses remotely.

In contrast, soft-magnetic composites respond in a very different manner to an external magnetic field. In soft MAPs, the magnetic particles have a null remanence magnetisation, therefore, under a null external magnetic field, these composites behave as traditional fillers with no functional response. However, under the application of a magnetic field with a given direction, these particles magnetise along such a direction. This last characteristic is one of the main distinctions to hMAPs. In this regard, the magnetisation of the particles in soft-magnetic composites always evolves with the direction of the external magnetic field. Therefore, there are no significant torques within the composite. Instead, the particles experience an increase in the magnetisation resulting into dipole-dipole interactions between particles. These interactions translate into attractive or repulsive forces leading to relative displacements of the particles. Similarly to hard-magnetic composites, these displacements find a mechanical resistance from the polymeric network. As a consequence, the soft MAP experiences a given deformation determined by a mechanical balance between polymeric network stress and particle-particle interactions, see Figure 4. It must be noted that, as the particles in hMAPs are initially magnetised, these also present dipole-dipole interactions that can vary during the deformation of the material. Therefore, apart from the internal torques, hMAPs also present some dipole-dipole interaction contributions to the overall magneto-mechanical responses. This last feature is extensively analysed and discussed in a recent work by the authors [21].

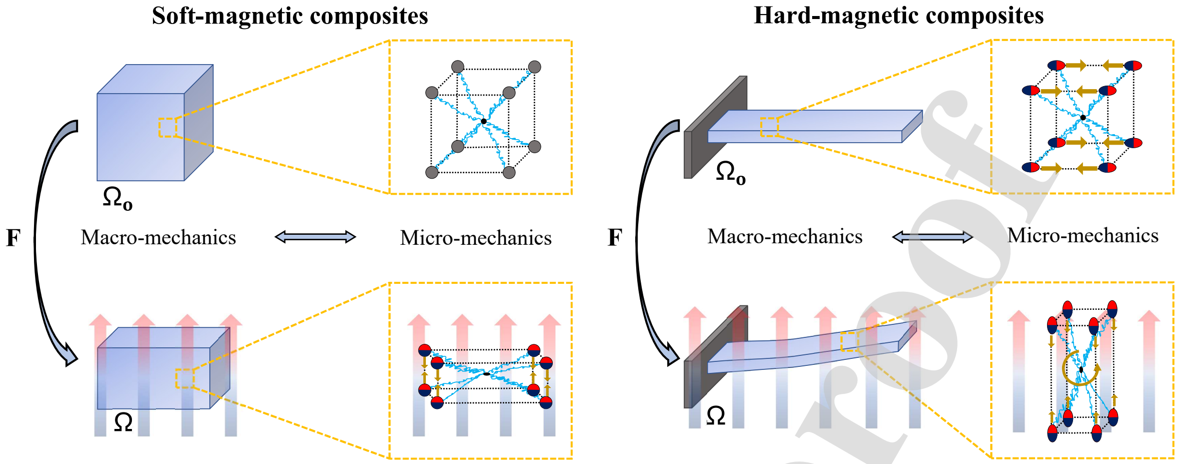

Figure 4. A schematic diagram of the MAP physics from macro- to micro-scales: soft-magnetic composites (left); hard-magnetic composites (right).

3.2. Magneto-mechanical fundamentals at finite strains

To date, different modelling approaches have been proposed to describe the magneto-mechanical response of hMAPs. A schematic classification of them is presented in Figure 5. These approaches can be divided into three main groups: microstructural-based models, continuum phenomenological models, and analytical models. Among the formers, full-field FE frameworks account explicitly for both matrix and particles phases to predict the coupled responses [38]. Such methods are computationally expensive but provide the most physical view of the problem. To provide efficient insight to describe the macroscopic response of the hMAPs while maintaining certain microstructural information, lattice-based models incorporate information on the particles' distribution into the constitutive formulations [21]. Then, among the continuum phenomenological models, the work by Kim and coauthors [4] stands out as one of the first approaches to this problem. This model defines the magneto-mechanical coupling by a dependence of the mechanical stress on the magnetic field, but without solving the magnetic problem (i.e., Maxwell's equations). Such a formulation has been recently completed by Mukherjee et al. [38] providing a microstructurally guided modelling framework accounting for full magneto-mechanical coupling including ferromagnetic hysteresis. Finally, we can find analytical models, mainly for slender beams, rods that can be used to predict specific structural configurations [25]. In the following, we introduce a general framework that supports the constitutive formulations of both magneto-mechanical models at the macro- and micro-scales. At first, the main features of finite deformation kinematics, magnetic variables, governing equations, and consistent derivation of constitutive equations are described. To this end, we provide a synthesis of the modelling fundamentals taking previous published works as references, e.g., [39, 40, 41, 42, 16, 14].

3.2.1. Kinematics and magnetic variables

Note that the hard-magnetic composite presents two phases with significant differences in their individual stiffnesses. In this regard, the polymeric matrix has a much lower stiffness than the magnetic particles. Therefore, under the application of mechanical loading, the hMAP deformation is mainly associated to the deformation of the polymeric network. Hence, as a homogenised composite, the mechanical response of a hMAP is primarily determined by the polymeric nature of the matrix, which leads to the capability of

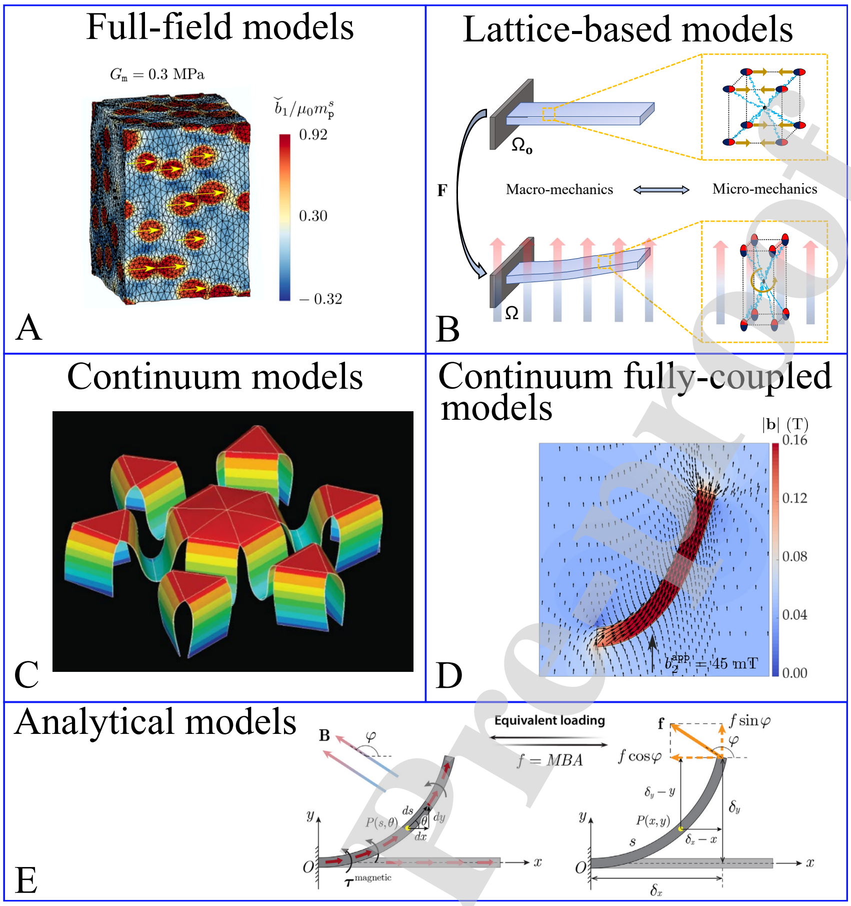

Figure 5. A schematic classification of the current approaches to model hard magnetics MAPs: A) full-field models consisting in FE frameworks where the polymeric matrix and the particles phases are explicitly defined [38]; B) lattice-based models consisting in continuum constitutive formulations informed with microstructural features of particles' arrangement [21]; C) continuum approaches defining the magneto-mechanical coupling by a dependence of the mechanical stress on the magnetic field, but without solving the magnetic problem (i.e., Maxwell's equations) [4]; D) continuum models considering full coupling between mechanics and magnetics [38]; E) analytical models for specific structural components (i.e., slender beams) [25].

deforming significantly resulting into significant geometrical changes. These large deformations make hyperelastic theory the ideal candidate to frame the constitutive formulation. Following these ideas, a material configuration Ω_0 is differentiated from the spatial configuration Ω. The coordinates expressed in Ω_0, $\boldsymbol{X}$, can be mapped to spatial coordinates in Ω, $\boldsymbol{x}$, through the nonlinear deformation map $\boldsymbol{\chi}$ which is in turn related to the deformation gradient $\boldsymbol{F}$ as

$$\boldsymbol{F} = \text{Grad}\,\boldsymbol{\chi}; \quad J := \det \boldsymbol{F} > 0. \tag{1}$$

The deformation gradient can be further used to define other tensorial forms representing the deformation state of the material such as the left and the right Cauchy-Green tensors $\boldsymbol{b}$ and $\boldsymbol{C}$, respectively, as

$$\boldsymbol{b} := \boldsymbol{F}\boldsymbol{F}^T, \quad \boldsymbol{C} := \boldsymbol{F}^T\boldsymbol{F}. \tag{2}$$

Regarding the magnetic field, it can be defined by three main magnetic variables: the magnetic field $\mathbb{h}$, magnetisation $\mathbb{m}$, and magnetic induction $\mathbb{b}$ in the spatial configuration; or, in the material configuration, $\mathbb{H}$, $\mathbb{M}$ and $\mathbb{B}$, respectively. These variables in two different configurations are related by

$$\mathbb{H} = \mathbb{h}\boldsymbol{F}, \quad \mathbb{M} = \mathbb{m}\boldsymbol{F}, \quad \mathbb{B} = J\mathbb{b}\boldsymbol{F}^{-T}. \tag{3}$$

In addition, these variables can be related in the bulk, as [43, 44]

$$\mathbb{B} = J\mu_0\boldsymbol{C}^{-1}[\mathbb{H} + \mathbb{M}] \quad \text{in } \Omega_0 \tag{4}$$

where, μ_0 is the relative permeability of the vacuum. However, some published works suggested that there is non-uniqueness of the Lagrangian form of $\mathbb{m}$ [15, 45, 43]. In addition, further works by Danas and coauthors [65] demonstrated that the pre-stretch does not affect the current magnetisation response, which is in agreement with experimental observations [46]. If these conclusions are followed, the constitutive relation in Eq. 4 is not considered and the magnitude of the magnetisation is assumed to not change with stretch ($\boldsymbol{U}$) but only with the rigid body rotation ($\boldsymbol{R}$) as [38, 21]

$$\mathbb{m} = \boldsymbol{R}\mathbb{M} \tag{5}$$

where, $\mathbb{M}$ is the initial magnetisation (residual or remanent magnetisation in hMAPs) expressed in the material configuration and $\boldsymbol{R} = \boldsymbol{F}\boldsymbol{U}^{-\mathbf{1}}$.

3.2.2. *Balance laws in the material configuration*

For the magnetic problem, the Maxwell's equations for magneto-statics are used as the governing equations. In the material configuration these are defined as

$$\text{Curl}\,\mathbb{H} = \mathbf{0}, \quad \text{Div}\,\mathbb{B} = 0, \tag{6}$$

where, Curl and Div are the corresponding differential operators with respect to the position vectors $\boldsymbol{X}$ in Ω_0. Note that if we derive $\mathbb{H}$ from a scalar potential φ, the governing equation $(6)_1$ is automatically satisfied, i.e.,

$$\mathbb{H} = -\text{Grad}\varphi, \quad \text{in } \Omega_0. \tag{7}$$

Moreover, the mechanical balance, related to the conservation of linear momentum, must be satisfied along with the angular momentum balance. In the material configuration, the linear momentum balance can be written as

$$\text{Div}\boldsymbol{P} + \boldsymbol{f}_0 = \rho_0\boldsymbol{a}, \quad \text{in } \Omega_0, \tag{8}$$

where $\boldsymbol{P}$ is the first Piola-Kirchhoff stres tensor, $\boldsymbol{f}_0$ is the external mechanical body force vector, ρ_0 is the material density, and $\boldsymbol{a}$ is the acceleration vector. Moreover, the angular momentum balance in hMAPs needs a special care, as the application of an external magnetic field can lead to an asymmetry in the Cauchy stress tensor, given by $\boldsymbol{\sigma} = \frac{1}{J}\boldsymbol{P}\boldsymbol{F}^T$, requiring [17, 42]

$$\varepsilon : \frac{\boldsymbol{\sigma} - \boldsymbol{\sigma}^T}{2} + \boldsymbol{\tau} = \mathbf{0}, \quad \text{in } \Omega, \tag{9}$$

where, ε is a third-order permutation tensor and $\boldsymbol{\tau}$ is the body torque generated by the magnetised domain under the application of an external magnetic field.

3.2.3. From thermodynamics to constitutive equations

Under isothermal conditions, the strain energy function (per unit reference volume) of the hMAPs can be expressed as a function of the deformation gradient ($\boldsymbol{F}$), a magnetic variable ($\mathbb{B}$ or $\mathbb{H}$), scalar internal variables (ξ) and vectorial or tensorial internal variables ($\boldsymbol{\xi}$) as

$$\Psi\left(\boldsymbol{F}, \mathbb{B}, \xi, \boldsymbol{\xi}\right) \quad \text{or} \quad \Psi\left(\boldsymbol{F}, \mathbb{H}, \xi, \boldsymbol{\xi}\right). \tag{10}$$

Usual scalar internal variables ξ are related to non-local damage problems, among others, and usual tensorial internal variables $\boldsymbol{\xi}$ are related to specific contributions of the deformation gradient to account for time-dependent viscous-relaxation mechanisms [14, 16]. Thus, the total energy in a magneto-mechanical problem, taking $\mathbb{B}$ as the magnetic variable, can be expressed as

$$\Omega(\boldsymbol{F}, \mathbb{B}, \xi, \boldsymbol{\xi}) = \Psi(\boldsymbol{F}, \mathbb{B}, \xi, \boldsymbol{\xi}) + M_0^*(\boldsymbol{F}, \mathbb{B}), \tag{11}$$

where, $M_0^*(\boldsymbol{F}, \mathbb{B}) := -\frac{1}{2J\mu_0}[\boldsymbol{C}\mathbb{B}] \cdot \mathbb{B}$ is the component associated to the free space in the material configuration. Considering the incompressibility condition for hMAPs, the second law of thermodynamics in the form of Clausius-Duhem inequality becomes [47, 48]

$$\begin{aligned} \delta_0 &= \boldsymbol{P} : \dot{\boldsymbol{F}} + p\boldsymbol{F}^{-T} : \dot{\boldsymbol{F}} + \mathbb{H} \cdot \dot{\mathbb{B}} - \dot{\Omega} \geq 0, & (12) \\ &= \boldsymbol{P} : \dot{\boldsymbol{F}} + p\boldsymbol{F}^{-T} : \dot{\boldsymbol{F}} + \mathbb{H} \cdot \dot{\mathbb{B}} - \frac{\partial \Omega}{\partial \boldsymbol{F}} : \dot{\boldsymbol{F}} - \frac{\partial \Omega}{\partial \mathbb{B}} : \dot{\mathbb{B}} - \frac{\partial \Omega}{\partial \xi} : \dot{\xi} - \frac{\partial \Omega}{\partial \boldsymbol{\xi}} : \dot{\boldsymbol{\xi}} \geq 0. & (13) \end{aligned}$$

The term related to p (a Lagrange multiplier associated to the pressure) is included to impose incompressibility [49, 50]. The constitutive equations can be consistently derived, applying the Coleman-Noll argumentation [47] as

$$\boldsymbol{P} = -p\boldsymbol{F}^{-T} + \frac{\partial \Omega}{\partial \boldsymbol{F}}, \quad \mathbb{H} = \frac{\partial \Omega}{\partial \mathbb{B}}. \tag{14}$$

The remaining terms associated to the internal variables, $-\frac{\partial \Omega}{\partial \xi} : \dot{\xi} \geq 0$ and $-\frac{\partial \Omega}{\partial \boldsymbol{\xi}} : \dot{\boldsymbol{\xi}} \geq 0$, establish consistency conditions to define the evolution of such internal variables.

3.2.4. Extension to modelling hydrogel-based MAPs

A special modelling scenario is the consideration of a hydrogel-based matrix for the MAP. Some important remarks must be done in this case due to the nature of the hydrogels. A hydrogel can be understood as a polymeric network within a given solvent can diffuse through. The local solvent concentration thus affects the volumetric deformation state of the polymeric network. Therefore, the mechanical response of the hydrogel is intrinsically coupled to the solvent diffusion process. This process can be modelled by the mass conservation law, in its material form, defining the rate equation for local change of solvent concentration as [51]

$$\frac{\partial c_{so}}{\partial t} + \text{Div}\, \boldsymbol{J_s} = r_s \quad in\ \Omega_o \tag{15}$$

where, $\boldsymbol{J_s}$ is the nominal flux of the solvent and r_s is a source term for the number of solvent molecules injected into unit reference volume per unit time. Similarly as done in Eq. 14, thermodynamic principles can be used to derive the constitutive expression relating the solvent concentration c_{so} with the solvent chemical potential μ_s as (see [14] for details)

$$c_{so} = -\frac{\partial \Omega}{\partial \mu_s}. \tag{16}$$

Note that to take into account the solvent diffusion process, the chemical potential μ_s must be incorporated as an independent variable in the definition of the total energy so that Eq. 11 now reads as $\Omega(\boldsymbol{F}, \mathbb{B}, \mu_s, \xi, \boldsymbol{\xi})$.

3.3. Macrostructural-based constitutive models

In last few years, motivated by the pioneering work advocated by Zhao and co-authors [4], the modelling of hMAPs has been approached by different authors. Most of these models follow the macroscopic approach developed by the same group in [17]. Such a phenomenologically-motivated model is formulated at finite deformations and is based on hyperelastic fundamentals. To this end, a total free energy per unit reference volume is defined as

$$\Psi\left(\boldsymbol{F}, \mathbb{B}\right) = \Psi^{\text{elastic}}\left(\boldsymbol{F}\right) + \Psi^{\text{magnetic}}\left(\boldsymbol{F}, \mathbb{B}\right) \tag{17}$$

where, $\Psi^{\text{elastic}}\left(\boldsymbol{F}\right)$ is a purely elastic mechanical contribution and $\Psi^{\text{magnetic}}\left(\boldsymbol{F}, \mathbb{B}\right)$ is a magnetic potential contribution. The elastic contribution can be defined following a neo-Hookean energy function as

$$\Psi^{\text{elastic}}\left(\boldsymbol{F}\right) = \frac{G}{2}\left[J^{-2/3} tr\left(\boldsymbol{F}^T\boldsymbol{F}\right) - 3\right] + \frac{K}{2}\left[J-1\right]^2 \tag{18}$$

with G and K being the shear and bulk moduli of the composite materials, respectively. The magnetic potential is defined assuming a residual magnetic flux density associated to the magnetic saturated particles that, expressed in the reference configuration, is denoted as $\mathbb{B}^r$. The magnetised particles are assumed to interact with an external applied field $\mathbb{b}^{\text{applied}}$ leading to a magnetic potential equal to

$$\Psi^{\text{magnetic}}\left(\boldsymbol{F}, \mathbb{b}^{\text{applied}}\right) = -\frac{1}{\mu_o}\boldsymbol{F}\mathbb{B}^r \cdot \mathbb{b}^{\text{applied}}. \tag{19}$$

The mechanical stress is then derived following the equivalent Eq. (14) for compressible materials $\boldsymbol{P} = \frac{\partial \Psi}{\partial \boldsymbol{F}}$. This approach was implemented for an idealised homogeneous magnetic field, defined by $\mathbb{b}^{\text{applied}}$. Therefore, no relevant perturbation of the magnetic field by the presence of magnetic particles is assumed and, then, the magneto-mechanical problem can directly be solved by computing the mechanical balance and defining the evolution of $\mathbb{b}^{\text{applied}}$ as an internal variable. This approach is totally valid when using particles with relative magnetic permeability close to 1 but, in the case of considering particles with a higher relative magnetic permeability, it needs to be extended to account for $\mathbb{b}^{\text{applied}}$ components as extra degrees of freedom.

This formulation has inspired other works that adopt such an approach to model different hMAPs structures. In this regard, Wang et al. [25] made use of this approach to develop a formulation that describes the analytical solution for hard-magnetic elastica under uniform magnetic fields. This theory was validated with FE simulations and experiments. A similar study was published by Chen et al. [52], where authors extended the theory to account for extreme bending deformations for beams. The same authors also extended the approach for functionally graded hard-magnetic soft beams [53]. Moreover, the work by Zhao et al. [17] was taking as starting point by Garcia-Gonzalez [42] to incorporate viscous effects in the response of hard-magnetic composites. Other recent works on the macroscopic modelling of hMAPs can be found in [54, 55, 56, 57].

Very recently, a new approach has been proposed by Ye et al. [58]. Therein, the authors developed a computational framework, called "Magttice", to model hMAPs by making use of the combination of FE scheme and lattice models. To this end, the effect of the external field on the magnetised particles is simulated by incorporating related nodal forces into a lattice model (pre-computed assuming uniform external magnetic field). Then, the complete model is implemented into an open-source molecular dynamics package, LAMMPS. This is further coupled to a Lattice Boltzmann method (LBM) to incorporate simulation techniques for multiphysics problems such as fluid-structure interactions. This work thus introduces some specific links with microstructural aspects. In the following section, different approaches that are directly linked to such microstructural features are presented.

3.4. Microstructural-based constitutive models

The different approaches that can be followed to address the modelling of hMAPs from microstructural bases can be divided into three main groups: lattice-based models, full-field models, and molecular dynamics formulations. The lattice-based models consist in incorporating specific features of the magnetic particles distribution within the constitutive formulation. Here, a given volume or finite element is approached from a representative lattice with an explicit definition of the particles' relative distances as well as the polymeric network surrounding them. Therefore, the constitutive formulation is defined as the combination of the microstructural contributions of the polymeric network and the magnetic particles. To the authors' knowledge, the first lattice-based continuum model accounting for a complete finite deformation formulation of hard magnetic composites is due to Garcia-Gonzalez and Hossain [21]. In this model, the total Helmholtz free energy function is devised as the contribution of mechanical (Ψ_{mech}) and magnetic (Ψ_{mag}) terms as

$$\Psi\left(\boldsymbol{F}, \mathbb{B}, \xi, \boldsymbol{\xi}\right) = \Psi_{\text{mech}}\left(\boldsymbol{F}, \mathbb{B}, \xi, \boldsymbol{\xi}\right) + \Psi_{\text{mag}}\left(\boldsymbol{F}, \mathbb{B}\right). \tag{20}$$

The mechanical contribution can be defined by the appropriate hyperelastic or visco-hyperelastic energy potentials depending on the specific material to be modelled. Moreover, the magnetic contribution is, in turn, divided into two terms

$$\Psi_{\text{mag}}\left(\boldsymbol{F}, \mathbb{B}\right) = \Psi_{\text{mag}}^{d-d}\left(\boldsymbol{F}\right) + \Psi_{\text{mag}}^{z}\left(\boldsymbol{F}, \mathbb{B}\right), \tag{21}$$

where Ψ_{mag}^{d-d} represents the magnetic potential related to dipole-dipole interactions and Ψ_{mag}^{z} represents the potential related to the hard-magnetic response (Zeeman potential energy, i.e., due to the application of an external field $\mathbb{B}$ on a magnetised solid). The magnetic potential per unit reference volume associated to the dipole-dipole interactions of the magnetisable particles can be defined in two different ways, depending on the given definition of the Lagrangian magnetisation vector $\mathbb{m}$. If the definition $\mathbb{m} = \mathbb{M}\boldsymbol{F}^{-1}$ is adopted, the potential is defined as (see, Garcia-Gonzalez and Hossain [16] for complete derivations and further details)

$$\Psi^{d-d}_{\text{mg}}\left(\boldsymbol{F},\mathbb{M}\right) = -\frac{\mu_o}{4\pi}\frac{\phi^2}{\gamma}\sum_{i=1}^{N}\left[\frac{3\left[\left[\boldsymbol{F}^{-T}\mathbb{M}\right]\cdot\left[\boldsymbol{F}\boldsymbol{R}_i^0\right]\right]\left[\left[\boldsymbol{F}^{-T}\mathbb{M}\right]\cdot\left[\boldsymbol{F}\boldsymbol{R}_i^0\right]\right]}{\left\|\boldsymbol{F}\boldsymbol{R}_i^0\right\|^5} - \frac{\left[\boldsymbol{F}^{-T}\mathbb{M}\right]\cdot\left[\boldsymbol{F}^{-T}\mathbb{M}\right]}{\left\|\boldsymbol{F}\boldsymbol{R}_i^0\right\|^3}\right] \tag{22}$$

Moreover, if the definition $\mathbb{m} = \boldsymbol{R}\mathbb{M}$ is adopted, the potential is defined as (see, Garcia-Gonzalez and Hossain [21] for more details)

$$\Psi^{d-d}_{\text{mag}}\left(\boldsymbol{F}\right) = -\frac{\mu_o}{4\pi}\frac{\phi^2}{\gamma}\sum_{i=1}^{N}\left[\frac{3\left[\left[\boldsymbol{R}\mathbb{M}\right]\cdot\left[\boldsymbol{F}\boldsymbol{R}_i^0\right]\right]\left[\left[\boldsymbol{R}\mathbb{M}\right]\cdot\left[\boldsymbol{F}\boldsymbol{R}_i^0\right]\right]}{\left\|\boldsymbol{F}\boldsymbol{R}_i^0\right\|^5} - \frac{\left[\boldsymbol{R}\mathbb{M}\right]\cdot\left[\boldsymbol{R}\mathbb{M}\right]}{\left\|\boldsymbol{F}\boldsymbol{R}_i^0\right\|^3}\right] \tag{23}$$

with N being the number of particles within the lattice, ϕ is the volume fraction of magnetic particles, $\boldsymbol{R}_i^0$ a dimensionless distance between particles, and the term γ being added to account for the number of particles per representative lattice selected (see, [59] for similar approaches).

In a similar fashion, the contribution of the hard-magnetic particles' interaction with the applied magnetic field can be defined, depending on the approach for the Lagrangian magnetisation vector, as

$$\begin{aligned}\Psi^{z}_{\text{mag}}\left(\boldsymbol{F},\mathbb{B}\right) &= -\boldsymbol{F}^{-T}\mathbb{M}\cdot\boldsymbol{F}\mathbb{B},\\ \Psi^{z}_{\text{mag}}\left(\boldsymbol{F},\mathbb{B}\right) &= -\boldsymbol{R}\mathbb{M}\cdot\boldsymbol{F}\mathbb{B}.\end{aligned} \tag{24}$$

Once the energy potentials are defined, the corresponding contributions to the mechanical stress can be directly derived following Eq. 14. In the recent work by Garcia-Gonzalez and Hossain [21], the authors numerically showed that the dipole-dipole interactions between hard-magnetic particles are especially relevant when modelling the mechanical response of the hMAP under null or low external magnetic fields. In addition, the authors discussed in detail some implications of such particles' interactions by mean of polymeric network pre-stretch and others.

Moreover, the micromechanical modelling of hMAPs can be tackled by the explicit definition of the composite phases (full-field models), i.e., the particles and the polymeric matrix. To this end, a representative volume element can be defined accounting for the geometry of the magnetic particles within the polymeric matrix explicitly. Specific constitutive equations can be defined for each phase. The polymeric phase is described by a hyperelastic energy function along with a low magnetic permeability, while the magnetic particles are defined as stiffer linear elastic solids with their corresponding magnetic permeability and remanent magnetisation. Then, the mechanical and magnetic balance equations are solved for the whole finite element domain imposing consistent periodic boundary conditions. A relevant work in the literature is due to Zhang et al. [60]. In this work, the authors study the effect of particles' rotation on the effective torque transmitted to the overall composite. In this regard, the shape and distribution of the magnetic particles were observed influencing the transmitted torque due to the application of an external magnetic field. Under such a scenario, the hard magnetic particles trend to align in the field direction leading to local shear deformation of the polymeric matrix as well as overall rotation of the composite. This modelling approach however presents certain limitations as no self-field magneto-mechanical coupling is accounted for (i.e., particles' interactions). A similar approach was published by Nadzharyan et al. [61], in which authors numerically studied the effect of magnetic field interactions with anisometric fillers on the surface deformation of hMAPs. Another relevant work is due to Kalina and co-authors [62], where they developed numerical simulations of hMAPs relating magnetic dissipation with microstructural rearrangements during the cyclic loading. Very recently, Mukherjee et al. [38] have developed a fully-coupled formulation providing a microstructurally guided modelling framework that also includes ferromagnetic hysteresis. In addition, equivalent approaches for soft magnetic composites have been developed by Zabihyan et al. [63, 64] and Mukherjee et al. [65].

Finally, a recent molecular dynamics approach to this problem is due to Sanchez et al. [66]. In this work, the authors studied the response of a polymeric matrix filled with a combination of soft and hard magnetic particles. Their results show that combining soft and hard particles can lead to either an elongation or a shrinking in the direction of the applied field depending on its magnitude. To conduct such an analysis, the authors developed a numerical framework based on molecular dynamics where they made use of equivalent magnetic potentials to Eqs. 22, 23 and 24 in order to describe the dipole-dipole interactions as well as the Zeeman potential energy. However, this work developed the formulation under infinitesimal strains and no influence of the deformation gradient in included is the magnetic terms. In addition, the elastic potential is defined by a linear elastic formulation. Following this work, Becker et al. [67] published a theoretical and experimental investigation on MAPs reinforced with mixed magnetic content. The problem is modelled by a mesoscopic approach of magnetic interactions between the hard- and soft-magnetic particles and numerically solved by using a FE framework under the assumption that the elastic matrix is rigid.

4. Applications of hard-magnetic soft composites

The ability of advanced fabrication techniques to integrate magnetic fillers in substrates of different nature opens up a wide range of possibilities for achieving complex functionalities on the final composites. The inclusion of hard-magnetic filler enables remote actuation capabilities to reproduce complex shape transformations due to mechanical torques arising from the interaction of the magnetised hMAPs with the external magnetic fields. The recent advances in magnetic soft materials and additive manufacturing technologies (see Section 2.1) make possible the design of sophisticated robots with complex capabilities, such as locomotion, jumping, crawling, bending, twisting, gripping, and releasing etc. Additionally, in the presence of soft-magnetic particles, alternating magnetic fields at high frequencies can be used for heat generation as a result dissipative behaviour of the composite. This allows for hyperthermia therapy, drug delivery and self-healing materials, suitable for the treatment of brain diseases such as strokes [68]. This section is intended to review past and current research on hard magnetic applications in soft composites. It is structured into subsections based on the types of applications, differentiating five main ones: smart actuators and sensors, soft robotics, biomedical applications, functional shape-morphing structures, and industrial components.

4.1. Smart actuators and sensors

The driving force mechanism is the alignment of the embedded hard-magnetic particles with the magnetic fields, generating torques that result in deformation, contraction, elongation, and bending. These forces can be created when the spatial gradients of the field interact with the magnetic particles or magnets. In small workspaces, magnetic fields and their spatial gradients can be generated independently. The actuation for complex motions can be achieved by the actuating magnetic torques and external forces. As magnetic fields can penetrate through a wide range of materials, these actuators are ideal candidates for working in enclosed confined spaces and are especially appealing for high force actuation mechanisms. Another advantage is their relatively fast response compared to other modes of actuations [69, 71, 70, 72]. Such features have led to magnetic soft actuators that allow for a variety of bending, gripper, and pumping actuators. Different deformation patterns can be designed by varying the actuating signals, the magnetisation profiles, and the overall shape and stiffness of the materials. In addition, the nature of these multifunctional composites can be used in a reversed manner, i.e., to sense mechanical alterations and translate them into electromagnetic signals. Few actuators made of hMPAs are briefly reviewed in the following section.

Figure 6. **A**: Bending response stages of hMAP cantilevered beam under an applied perpendicular magnetic field [75]. **B**: Design and magnetisation profile of a four-arm magnetic shape memory hMAP gripper. Lift of a lead ball with and without shape locking under the application of different magnetic fields [78]. **C**: Robotic six-DOF soft hMAP gripper assembly of a 3D four-bar linkage device by controlling the magnitude of the magnetic field producing grabbing, transporting, and releasing motions [86]. **D**: Remotely-actuated untethered micro-gripper designs. (a-c) Torque-based addressable micro-gripper that exerts a torque under a constant uniform magnetic field. (d–f) Force-based addressable micro-gripper where the gripping state is changed through the application of a large magnetic field pulse, which switches the ferrite magnet magnetization directions. (c,f) Scanning electron microscope (SEM) images of a fabricated grippers. (g) Magnetic coil system used to apply low and moderate fields. (h) Normalized magnetisation hysteresis loops of NdFeB and ferrite magnetic materials [80]. **E**: Photographs of a hMAP rotor of the untethered pump where the driving mechanism consists of a pair of permanent magnets and a rotating electric motor [93]. **F**: Illustration of the nanocomposite cilia tactile sensor. The sensor is made of permanent magnetic nanocomposite cilia integrated on a magnetic sensor that mimics the neuron in natural cilia. When the cilia get deflected by external forces such as fluid flow or hand touch, the stray field at the magnetic sensor changes, which also changes its impedance [96]. **G**: Array of compliant magnetic microelectromechanical system sensors [97]. (a) Schematic illustration of a 2 x 2 array. (b) Photograph of a free-standing sensors array. (c) A multi-pixel sensor conformally adhered onto a model finger. (d) Sensitivity of the four pixels when consecutively pressed with a cotton swab. (e) Sensitivity of the four pixels on the array when approached individually by a cylindrical soft magnet.

4.1.1. Bending actuator

One of the simplest functional applications of magneto-composites is the actuation by a bending motion. This can consist of a hMAP cantilevered beam that, when uniform magnetic fields are applied perpendicularly to the polarized direction, experiences a rotational motion aiming to align the magnetised particles with the external field (Figure 6A). The conceptualisation of such actuators has been tested in [74, 75], in which the authors show a linear relation between the beam deflection and the blocked force at the tip over a reasonable range. These results suggest the use of hMAPs as bending-type actuators in small mechanical systems and devices. In a similar fashion, an elastic magnetic bar filled with permanently magnetised Sm_2Co_7 micro-particles has been proven valid for very ductile actuator systems [73]. A recent study [76] evaluates the influence of the polymeric matrix stiffness for these systems. To this end, a novel mould-free fabrication procedure controlling the crosslinking degree is presented leading to different stiffness of hMAPs. Thus, the mechanical properties of MAP matrices can be controlled to optimise the performances of membrane actuators. An alternative for more complex actuators is due to Song et al. [77], which is based on a multifunctional composite containing magnetic microspheres encapsulated with an oligomeric polyethylene glycol. This new methodology allows for rewriting the magnetisation profiles of the composite by physically realigning the ferromagnetic particles and controlling the encapsulating polymer phase transition, yielding into diverse magnetic actuators with reprogrammable complex magnetisation.

4.1.2. Gripper actuator

Advances in soft robotics, materials science, and stretchable electronics have enabled rapid progress in manufacturing of soft grippers. One of the most important applications of the hMAPs is the remotely triggered grippers [83, 84, 85]. Under the application of a magnetic field, the hard magnetic particles with programmed domains exert micro-torques leading to a large macroscopic shape change (Figure 6B, 6C and 6D). In this regard, Diller et al. [80, 81, 86] introduced a flexible patterned magnetic material which allows for internal actuation, resulting in a mobile micro-gripper which is driven and actuated by magnetic fields. By remotely controlling the magnetisation direction of each micro-gripper arm, they were able to control the gripping motion which can be combined with the locomotion for precise transport, orientation, and programmable three-dimensional assembly of micro-parts in remote environments. In [79], magnetically driven bionic actuators based on hMAPs have been developed to achieve some specific functions in different fields. For instance, under the control of the applied magnetic field, the bionic actuators not only generate time-varying deformations but also create motion in diverse environments, suggesting new possibilities for the target gripping and directional transporting, especially in the field of soft robots and biomedical engineering.

In practical applications, it is highly desirable that the actuated shape can be locked with high enough stiffness so that the material can fulfil certain functions requiring high supporting or self-supporting force without the constant presence of an external stimulation. In [78], a novel magnetic shape memory composite is reported as a locking mechanism. The composite consists of the combination of two types of magnetic fillers within an amorphous shape memory polymer matrix. The matrix softens via the magnetic inductive heating of low-coercivity particles, and high-remanence particles while reprogrammable magnetisation profiles of the hard magnetic particles drive the rapid and reversible shape change under actuating magnetic fields. Once cooled, the actuated shape can be locked. Moreover, an extension of the capabilities of the aforementioned mobile untethered microgrippers was presented in [82]. Using simple control strategies, three-dimensional micro-grasping and cargo delivery of a microgripper was demonstrated. The developed microgripper and controller allow to reliably grasp and transfer micro-objects, such as cells, with minimal user input, which is ideal for cooperative tasks performed by multiple microgrippers. For more magnetic gripper actuators the works in [87, 88, 89, 90, 91, 92] are referenced.

4.1.3. *Pumping actuator*

The last type of actuator presented herein is consisting of pumping devices that can be controlled remotely. One of the first approaches for pumping actuator is due to Mitsumata et al. [93]. In this work, a gel-matrix made of sodium alginate or poly(vinyl alcohol) was filled with hard magnetic barium ferrite particles, thus leading to a multifunctional composite in the form of a flexible fluid pump [93]. This pump consists of a magnetic screw-shaped gel-rotor and a driving magnet, as shown in Figure 6E. Rotational motion can remotely be imposed on the rotor by a magnetic field generated from the driving magnet, resulting in an efficiently delivery of high water flows in straight and spiral tubes. Another approach presented in [94] consisted in the development of a valveless electromagnetic micropump with a hard magnetic polymer composite (PDMS) actuator membrane structure, fabricated using a soft lithography process. The magnetic membrane was integrated with a microfluidic system and functionally tested, showing a great potential to improve the injection accuracy of the drug dosage and the proficiency of the existing drug delivery system.

4.1.4. *Remote sensors*

Aside from the use of hMAPs in high force actuators, they can be used as low power consumption sensing devices. For instance, Becker et al. [95] investigated the material properties and motion behaviour displayed by hMAP beams in the presence of a uniform magnetic field, where it is demonstrated that the deflection of the beam can be identified unambiguously by magnetic field distortion measurements. A multifunctional biomimetic nanocomposite tactile sensor was developed in [96] to detect shear and vertical forces, feel the texture, and measure flow (see Figure 6F). On the top of the magnetic multilayer giant magneto-impedance sensor, permanent magnetic and highly elastic nanocomposite cilia structures were manufactured serving as a biomimetic tactile sensor. The permanent magnetic properties of the nanocomposite are achieved by using ferromagnetic nanowires (with high coercivity and biocompatibility). These, in turn, generate a stray field, as a function of the cilia deflection, that is detected by a magneto-impedance sensor. Similarly, Ge et al. [97] developed a bifunctional electronic skin equipped with a compliant magnetic microelectromechanical system that is able to transduce both mechanical pressure and magnetic fields stimulations simultaneously enabling complex interplay with physical objects enhanced with virtual content data in augmented reality, robotics, and medical applications.

In the work of Almansouri et al. [98], a biocompatible magnetic skin is introduced offering extreme flexibility, stretchability and lightweight, while maintaining a remanent magnetisation. Combined with magnetic sensors, its tunable magnetic properties can be customised to provide remote control functionalities. Eye-tracking and remote gesture tracking are some examples that open the door to new control concepts, relevant for people with disabilities, sterile environments, or the consumer industry. Alternatively, composite materials containing embedded magnetic wires [99, 100] are able to change the electromagnetic response in a desirable way providing information about the material properties (e.g., stress, strain, temperature). The strong field dependence of the effective permittivity of these composites postulates them as candidates for a wide range of self-sensing applications.

4.2. *Soft robotics*

The ability of hMAPs to achieve manipulation and guidance of soft actuators makes them one of the most suitable materials for soft robotic devices. Soft robotic systems have characteristic compliance that allows for continuous and responsive localised deformations. These smart composites have been employed to construct contactless programmable soft robots that are able to realise complex remote manipulation and repeatable movements, such as rolling, twisting, and folding under the external stimuli of magnetic fields

[103, 102]. Therefore, soft robots are especially interesting for their integration with human tissues. In this regard, MAP-based soft robots can be designed in the form of biomedical devices, as well as to provide remotely activated performances in harsh or uncertain environments, such as the exploration in small confined spaces or locomotion on abrupt terrains. Additionally, miniaturised applications are also found for biomedical purposes such as nanorobots or microswimmers [106, 101, 104, 105].

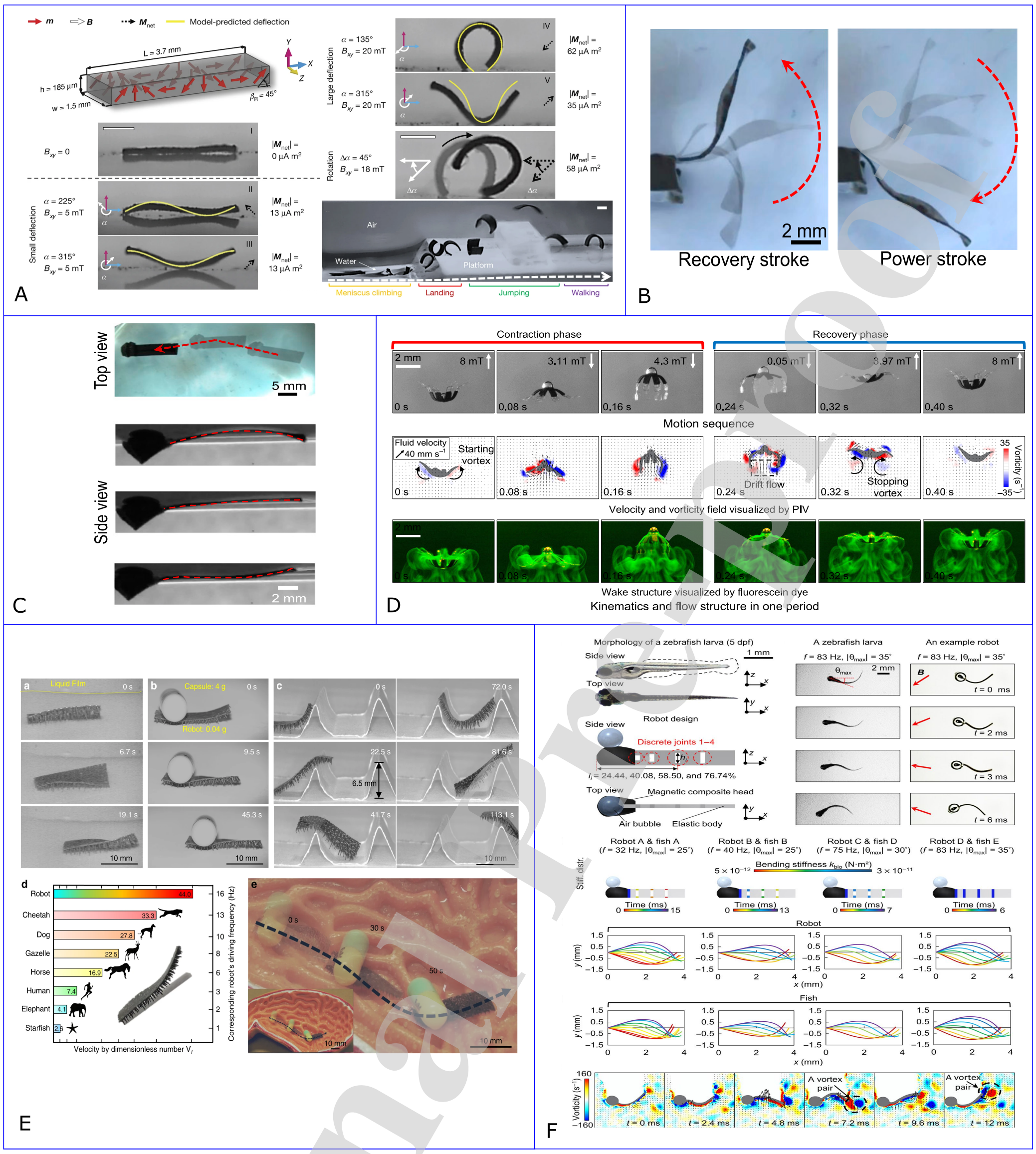

Figure 7. **A**: Design, shape-change mechanisms, and rigid-body rotation of the magneto-elastic soft multimodal locomotion of hMAP millirobot under different applied magnetic fields. Swimming, climbing, and obstacle jumping over a hybrid liquid–solid environment [11]. **B**: Magnetically activated artificial hMAP cilium motion where a specific magnetisation profile has been programmed to optimise the bending moment: power and recovery strokes [18]. **C**: Spermatozoid-like undulating hMAP soft swimmer. Snapshots extracted from the motion of the undulating swimmer swimming on an air–water interface—top view and side view of the swimmer [18]. **D**: Design and swimming behaviour of the jellyfish-inspired swimming soft millirobot: Kinematics and flow structures achieved by biomimetic motion mode. The motion sequence, the velocity and vorticity fields, and the wake structures visualized by the fluorescein dye are all in one cycle [3]. **E**: Demonstration of hMAP untethered soft millirobot locomotion at harsh environment activated [12]. (a) Locomotion on wet surface with liquid film. (b) Robot locomotion with a loading 100 times of its own weight. (c) Cross a steep obstacle with height 10 times higher of its own leg. (d) Comparison of the normalized speed between the soft robot and other animals. (e) Demonstration of drug transport in a stomach model under harsh wet in vivo simulated environment carrying a medical tablet twice heavier than itself. **F**: Larval zebrafish–like, untethered undulatory soft millirobot design. Morphology of a zebrafish larva. A comparison of kinematics between a fish and a robot in half period during near-cyclic swimming with different orientation of the magnetic flux density. Designs of bioinspired robots to capture the biological midline kinematics and simulations of the wake flow patterns [126]

4.2.1. *Soft robot locomotion*

Soft robots are capable of mimicking the complex motion of animals. By carefully designing the geometry and magnetisation direction of the hMAP components, locomotion can be controlled by the repeated application of the external magnetic field. Regarding this application, in the works of [108, 107] pioneer untethered micro-robots were fabricated by molding process of magnetic-powder-impregnated polyurethane, capable of locomoting on 2-D surfaces. Tasoglu et al. [113] described a method to code soft hydrogels, rigid copper bars, polystyrene beads, and silicon chiplets into three-dimensional heterogeneous structures to develop untethered magnetic microrobots. Other authors have proposed alternative manufacturing methods to design robots by photolithography techniques [115, 114]. These consist of a polymeric body with two sections with embedded magnetic particles aligned at the ends, and a middle non-magnetic bridge region. Such a microscale magnetic tumbling robot is capable of traversing complex terrains in dry and wet environments. Additionally, Zhang et al. [116] used magnetic microparticles embedded into a liquid crystal elastomers film and, taking advantages of both materials without compromising their independent stimuli-responsiveness, developed an untethered in situ reconfigurable soft miniature machine that self-adapts to different environments/terrains by exhibiting distinct locomotion modes.

The advances in 4D printing techniques have revolutionised the field allowing for programming mechanical responses to external magnetic fields. Shinoda et al. [110] used an UV-curable lithography gel material to manufacture biomimetic examples such as a worm-type soft actuator. Multiple planar microrobots with various sizes and geometries, arbitrary magnetisation profiles were fabricated in [85] (see Figure 8G). By a 3D complex magnetisation profile, higher-order and multi-axis bending, large-angle bending, and combined bending and torsion were achieved enabling shape changes and microrobotic locomotion mechanisms such as multi-arm power grasping and multi-legged paddle crawling. In [12, 79], an untethered soft millirobot decorated with multiple tapered soft feet architecture was fabricated using a modified magnetic particle assisted moulding of a mixture containing polydimethylsiloxane (PDMS), hexane, and magnetic particles. Such robot design yields superior adaptivity to various harsh environments with ultrafast locomotion speed, ultra-strong carrying capacity, and excellent obstacle-crossing ability (see Figure 7E).

Moreover, multimodal locomotion enables different types of actuation including jumping, rolling, crawling, and walking of an inchworm (see Figure 7A). The ability of magneto-elastic soft millimetre-scale multimodal robots to swim inside and on the surface of liquids, climb liquid menisci, roll and walk on solid surfaces, jump over obstacles, and crawl within narrow tunnels was demonstrated by [11, 111]. The microscale robots can transit reversibly between different liquid and solid terrains, as well as switch between locomotive modes, in addition to executing pick-and-place and cargo-release tasks. Alapan et al. [109] carried out tunable locomotion of a surface-walking soft robot by using a heat-assisted magnetic programming strategy enabling a rich design space and mass-manufacturing capability for development of multiscale and reprogrammable soft machines. Wu et al. [112] developed an evolutionary algorithm (EA)-based design strategy to achieve the desired magnetic actuation and motion with complex geometry variations and curvature distributions in a voxel-encoding direct-ink-write printing domain. The proposed algorithm for the guided voxel-encoding direct-ink-write printing method significantly broadens the application potentials of hMAPs for advanced applications such as biomimetic motions. For more magnetic soft robots examples see [120, 119, 117, 90, 118]

4.2.2. *Soft swimming robots*

A breakthrough in soft magnetic robots, that is not provided by conventional rigid robots, is their ability to achieve superior performance under both wet and dry conditions. To accomplish this, some works have proposed solutions that can generate a true travelling-wave deformation along the length of its body [124, 121]. To this end, these robots present a spatially-varying magnetisation profile within a flexible sheet that reacts under the application of an external rotating magnetic field. This flexible sheet was manufactured by pressing the mixture of a soft silicone matrix such as Ecoflex and magnetic particles between two glass slides during the curing process, forming a millimetre-scale magnetically driven swimming robot for untethered motion ranging from mid to low Reynolds numbers.

Moreover, different micro- or millirobots that follow biomimic designs can be found in the literature. For example, in [122], a single-hinge microswimmer is reported, which propels in shear thickening and shear thinning fluids by a reciprocal motion. In [125], a miniature swimming robot design with multiple flexible artificial flagella is introduced. In this case, a two-step photolithography-based microfabrication (e.g., two-photo polymerisation) method is proposed to handle more complex flagella designs. More recently, a two-step moulding process was used in [18, 3] to embed a heterogeneous programmed distribution of hard ferromagnetic and aluminium microparticles into a silicone rubber. Whereas the fabrication technique is generic only for creating magnetisation profiles on planar beams, a vast number of miniature soft devices can be designed. Based on the magnetisation programming method, a jellyfish-like robot, a spermatozoid-like undulating swimmer, and a zebrafish-like swimmer (see Figures 7C, 7D and 7F), which mimic the complex beating patterns of some biological creatures, were produced. In a similar manner, 3D printed moulds of PDMS with NdFeB particles were used to design multimodal deformation, untethered biomimetic swimming robots that provide an effective propulsion mechanism in [111], yielding into fast-transforming actuation robots such as a four-leg swimming robot and a swimming frog. Very recently, a magnetic soft robot made of hard ferromagnetic microparticles embedded into a silicone rubber, with the triangular head-tail morphology and sine-based magnetisation, was developed by Manamanchaiyaporn et al. [123]. The magnetic-elastic robot utilises a high degree of freedom provided by the magnetic compliance for the mobility in a form of lateral undulation, similar to the movement of an eel or a snake. More examples of soft swimming robots can be found in [127, 128, 129]

4.2.3. Artificial cilia

Cilia are tiny hair-like structures that cover the surfaces of biological cells, being flow generation is one of their main functions. Artificial cilia are mechanical actuators that are designed to mimic the motion of natural cilia to create fluid transport in microchannels. These fluid propulsion systems have good potential for application in lab-on-a-chip devices to be used in, e.g., point-of-care diagnosis. Lum et al. [18] created an artificial soft cilium that was able to approximate the complex beating pattern of a biological cilium by programming the magnetisation profile in a silicone rubber filled with hard magnetic microparticles. This beating pattern was divided into two strokes: the power and the recovery ones (see Figure 7B). Furthermore, an array of artificial cilia was presented in [110] employing an UV-curable gel and applying a magnetic field to set magnetic anisotropy in the curing portion during the building step. This anisotropy was set in each region so that the printed structures could deform under an applied magnetic field, enabling the artificial cilia to reproduce a metachronal wave, which is a phase propagation wave found in small organisms from nature. Similar cilia structures were developed in [130] using two-step moulding on 3D printed polymeric structures mixed with NdFeB particles. By stretching and folding onto curved templates, programmable magnetisation patterns were encoded into artificial cilia carpets, which exhibit metachronal waves in dynamic magnetic fields. In [132], by curing a mixture of silicone rubber and NdFeB microparticles, soft miniature devices were fabricated with both ciliary nonreciprocal motion and metachronal coordination to investigate the quantitative relationship between metachronal coordination and the induced fluid flow.

4.3. Biomedical applications

Probably the most promising fields for hard-magnetic soft composites are the biomedical and bioengineering areas. Rapidly expanding novel methods in 4D printing techniques to manufacture such materials have opened the door by overcoming the past bottlenecks with significantly advancements in the sector. In this regard, even a tiny smart system can be developed to provide specific functionalities across the different biological scales [133]. In addition, biological tissues posses low magnetic permeabilities so that they do not create important perturbations in the magnetic fields. This feature is essential to allow for remote activation and control of intricate magneto-active devices and opens the route for designing novel applications even accessible to confined biological regions. For more magnetically activated boimedical applications see [134, 135, 136, 137, 138, 139]

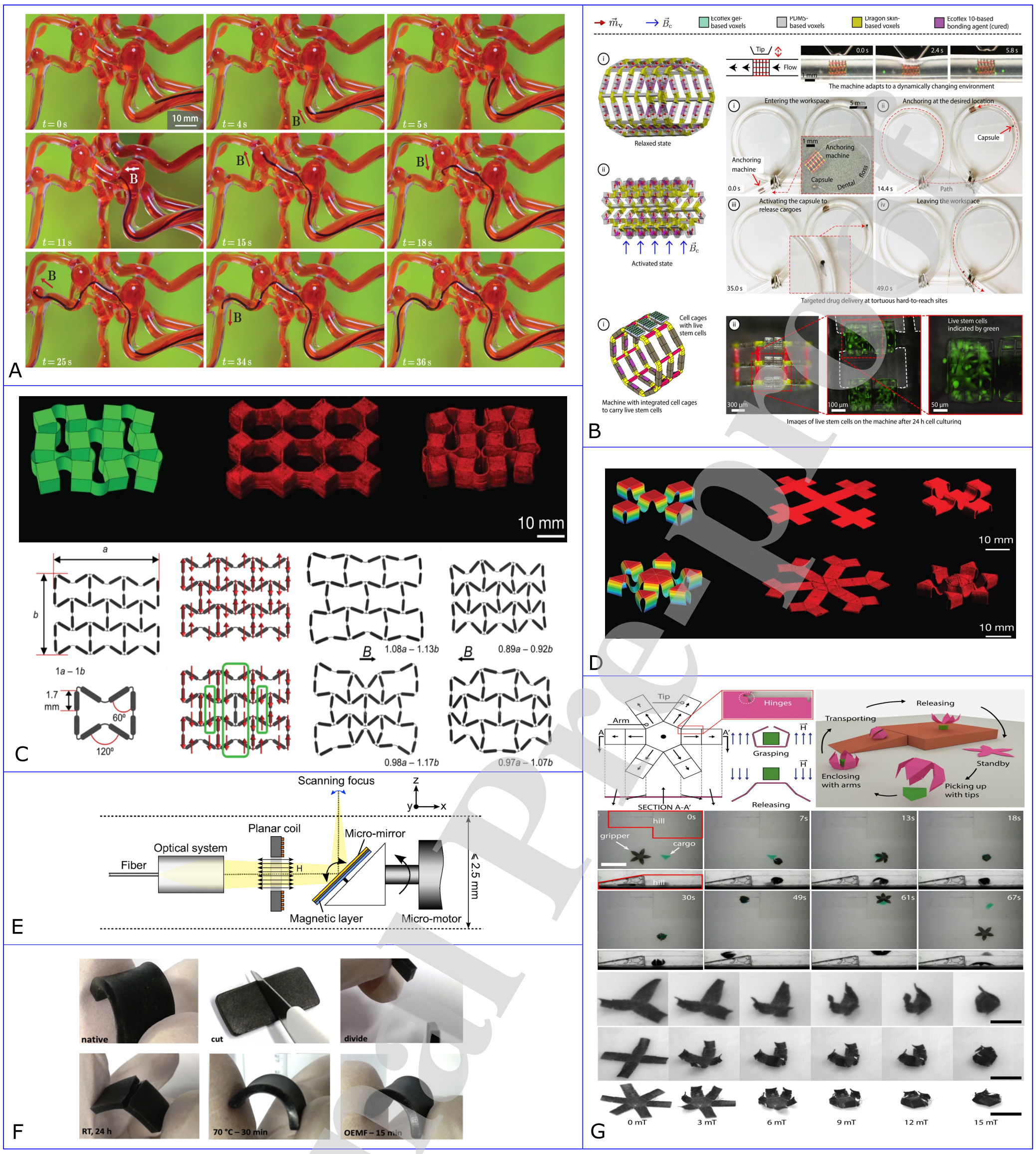

Figure 8. **A**: Demonstration of navigating through a 3D cerebrovascular phantom network of a magnetic soft continuum robot [10]. **B**: Wireless miniature magnetic soft anchoring machine with potential biomedical functionalities. (Top) Surface-anchoring machine anchoring and releasing: relaxed and activated states. Anchoring and cargo delivery demonstration in a synthetic tube with a fluid (water) flow: Machine locomotion, relaxing at the desired location and capsule activation to release the liquid cargo (dye here). (Bottom) Live stem cell integrated machine demonstration toward future vascular regeneration applications. Microcages containing cells and zoomed fluorescence optical images, taken 24 hours after the cell culturing. **C**: Finite-element simulations and experimental results for hMAP auxetic structures (with negative Poisson's ratios) exhibiting shrinkage in both length and width under applied magnetic fields [4]. Tuning mechanical behaviour of an auxetic metamaterial by reprogramming the distributed magnetization profile of individual units. The flexible auxetic structure expands and compresses both in length and width depending on the magnetic actuation direction [109]. **D**: 2D quadrupedal and hexapedal 3D printed hMAP structures enabled by folding of the magnetically active segments surrounding the magnetically inactive segments [4]. **E**: Schematic sketch of a tubular scanning endoscopic probe. The magnetic micromirror is rotated by an integrated micromotor about the x-axis while it delivers a fast 1-D scan, yielding in combination a 2-D tubular scan [144]. **F**: Illustration of cut and heal experiments of a self-healing hard-soft particle filled polymer [151]. **G**: Untethered multi-arm magnetic micro-robot for transportation: geometry, magnetization profile, illustration and images of the cargo transportation task. Images of magnetic microgrippers that have a configurable number of arms to target various cargos shape at different magnetic field levels [85].

4.3.1. *Artificial muscles*

The ability of hMAPs to undergo large strains in response to an external magnetic field has motivated the development of high deformation actuators in the form of artificial muscles. These devices can exert a strong contraction behaviour activated by an external magnetic field, resulting in a significant shape change. One of the key ideas to conceptualise such multifunctional structures is torsional actuations originated from the volumetric expansion of twisted structures [140]. Recently, Lee et al. [140] developed a smart textile in the form of helical yarns composed of carbon nanotubes accompanied with NdFeB nanoparticles. Under the application of an external magnetic field, these yarns actuate generating torsional forces leading to rotations up to 80°. This actuation method can be applied over extreme temperatures in vacuum, air, explosive, inflammable, or corrosive environments.

4.3.2. *Biomedical navigation*

Small-scale magnetic soft robots capable of active steering and navigation may open avenues to minimally invasive robotic surgery for previously inaccessible lesions, thereby addressing challenges and unmet needs in the healthcare sector. Recently, a new type of slender, thread-like hard-magnetic soft robots that can be steered magnetically, has been developed by Kim et al. [10, 25]. Composed of soft polymers with embedded hard-magnetic particles as distributed actuation sources, ferromagnetic soft continuum robots produce large-scale elastic deflections through magnetic torques and/or forces generated from the intrinsic magnetic dipoles under the influence of external magnetic fields. These robots have shown their capability to navigate through complex and constrained environments, such as a tortuous cerebrovascular phantom with multiple aneurysms (Figure 8A). In the work of Zang et al. [143], a bottom-up assembly-based 3D microfabrication approach to create complex 3D miniature wireless magnetic soft machines at the milli- and sub-millimeter scale with arbitrary multimaterial compositions, arbitrary 3D geometries, and arbitrary programmable 3D magnetisation profiles at high spatial resolution is presented. This technique enables complex biomedical device-related functionalities, including peristaltic pumping of biological fluids and transport of solid objects, active targeted cargo transport and delivery, liquid biopsy, and reversible surface anchoring in tortuous tubular environments withstanding fluid flows (Figure 8B).

4.3.3. *Biomedical scanners*

Hard magnets can be used for mirroring and deflection of magnetic resonance scanners. However, the placement of large-sized magnets hinders the very localised scanning. In [144], extremely compact hard-magnetic micromirrors were realised using a combination of silicon and polymer microelectromechanical systems (Figure 8E). Due to their hard-magnetic properties, the mirrors can achieve high deflection angles with the application of very low magnetic fields, which can be generated by means of miniaturised micro-coils. Since no electrical wiring is required for the mirrors, they may be mounted on rotating platforms and thus used for complete circumferential scanning, as required, for example, in optical endoscopic diagnostics.

4.4. *Shape-morphing and self-healing structures*

The properties and functionalities of hMAPs are related to the configurations and deformations inherent to the structures. They are capable of transforming complex three-dimensional shapes in response to magnetic fields, offering a safe, fast, remote, and effective manipulation method, even in enclosed and confined spaces. Such hMAPs for complex shape-morphing show applications for biomedicine, flexible electronics and soft robotics. In addition, the presence of magnetic particles in these structures not only allows for controlling changes in shape, but also for recovering the structural integrity mimicking bioinspired processes.

4.4.1. Complex shape-morphing structures

With advances in the magnetic field control, magnetically responsive soft materials have also evolved from embedding discrete magnets or incorporating magnetic particles into soft compounds to generating non-uniform magnetisation profiles in polymeric sheets. Kim et al. [4] reported a 3D printing direct ink writing method of programmed ferromagnetic domains in soft materials that enables fast transformations between complex 3D shapes via a magnetic actuation. This method allows to program ferromagnetic domains (Fig. 8D) with a set of previously inaccessible modes of transformation used for complex shape changes and reconfigurable soft electronics. Alapan et al. [109] used a heat-assisted magnetic programming strategy establishing a rich design space and mass-manufacturing capability for the development of multiscale and reconfigurable shape-morphing structures. Additionally, origami-inspired structures have been studied in [145]. The magnetically responsive origami systems enhance the shape-changing capability for multifunctionality with applications leading to tunable, deployable, and multifunctional systems including robotics, morphing mechanisms, biomedical devices, and outer space structures.

4.4.2. Metamaterials

Mechanical metamaterials are architected structures that allow for unique behaviours not observed in nature, making them promising candidates for a wide range of applications. Existing metamaterials demonstrate some limitations due to their lack of tunability which considerably restricting the changes in properties after their fabrications. However, metamaterials made of hard-magnetic fillers can offer integrated multifunctional shape manipulations including reprogrammable, fast and reversible shape transformation and structure locking. In [4, 111], lattice structures for stimuli responsive metamaterials are presented (see Figure 8C). These designs are able to extend the 2D phase space to 3D through rapidly and repeatedly switch signs of constitutive parameters with remote magnetic fields. It is shown that effective modulus can be reversibly switched between positive and negative within controlled frequency regimes through lattice buckling modulated by magnetic fields. This novel concept opens promising avenues for remote, rapid, and reversible modulation of acoustic transportation, refraction, imaging, and focusing in sub-wavelength regimes. Very recently, reconfigurable mechanical behaviour of auxetic metamaterial structures has been reported in [109]. They proposed a high-throughput magnetic programming strategy based on heating magnetic soft materials above the Curie temperature of the embedded ferromagnetic particles. Then, magnetic domains are reoriented by applying magnetic fields during cooling. A reconfigurable mechanical behaviour of an auxetic metamaterial structure was demonstrated using the reprogrammable magnetisation capability (Figure 8C).

Another interesting application of multifunctional metamaterials is acoustic isolation. Inspired by the sharkskin denticles, Lee et al. [148] presented a class of active acoustic metamaterials whose configurations can be on-demand switched via untethered magnetic fields. This approach enables active switching of acoustic transmission, wave guiding, logic operation, and reciprocity. The magnetically deformable resonator pillar arrays, made of a magneto-active elastomer, can be tuned between vertical and bend states corresponding to the acoustic forbidding and conducting, respectively. In [147], the architecture of this metamaterial employs an asymmetric joint design using hMAPs that permits two distinct actuation modes (i.e., bending and folding) under oppositely oriented magnetic fields. The subsequent application of mechanical compression leads to branching deformation mode, where the metamaterial architecture transforms into two distinct shapes. These shapes exhibit very different deformations and enable great tunability in properties such as mechanical stiffness and acoustic bandgaps. Similarly, in [143], using 3D microfabrication approach metamaterials with programmable shape morphing, negative Poisson's ratio, complex stiffness distribution, directional joint bending, and remagnetization for shape reconfiguration are achieved.

Furthermore, metamaterials design can be incorporated in magnetic shape memory polymers for global stiffness tunability, which also allows for the global shift of the acoustic behaviours. In the work of Ma et al. [56], multimaterial printing technology is developed for the complex structural integration of magneto-active shape memory polymers to explore their enhanced multimodal shape transformation and tunable properties by incorporating thermal and magnetic actuation. Recently, Chen et al. [149] proposed a novel metamaterial design that comprises an array of physical binary elements (m-bits), analogous to digital bits, with clearly delineating writing and reading phases. Each m-bit can be independently and reversibly switched between two stable states (acting as memory) using magnetic actuation to move between the equilibrium of a bistable shell. The stable memory and on-demand reprogrammability of mechanical properties in the proposed design paradigm will facilitate the development of advanced forms of mechanical metamaterials.

4.4.3. Self-healing structures

Autonomous or on-demand self-healing characteristics in flexible and elastic materials is a desirable property in many functional applications. Self-healing materials can reverse mechanical damage by activating self-repair mechanisms, similar to a biological process [150]. The self-healing effect in dynamic systems is accelerated by heat or stress which principally can be brought in from different energy sources such as UV- or IR irradiation and conventional heating. Although most of the magneto responsive composites are formed by soft magnetic particles, Hohlbein et al. [151] designed hMAPs that make use of energy dissipation and the associated heating. Therein, the heat energy is arising as a result of interactions between hard and soft magnetic nanoparticles with alternating electromagnetic fields, thus locally accelerating the self-healing behaviour in acrylate-based elastic ionomer (see Figure 8F). The local inductive heating of magnetic particles considerably accelerates the healing process when material dynamic crosslinks are thermally reversible. The remotely activated self-healing materials offer different advantages: contactless, remote-controlled trigger, local effect, and high efficiency. These systems are especially interesting for applications in environments with difficult access and replacing.

4.5. Industrial components

4.5.1. Vibration isolation: dampers

The controllable properties of the hard-magnetic soft composites enable the design of tunable vibration isolator devices. Within the field of vibration damping and control, the combination of polymers with magnetic particles provide enhanced properties compared to the traditional materials for vibration absorbers. Most magneto-active soft composites for dumping are based on magnetically soft fillers like carbonyl iron particles. However, in [152], authors studied magnetic field sensitive elastomers filled with both soft- and hard-magnetic fillers, enabling the tuning of the elastic modulus by an external magnetic field. Similar studies are due to Stepanov et al. [153], where silicone polymer matrices are filled with NdFeB-alloy magnetic particles. The viscoelastic properties of the hMAP and, therefore, its damping properties, can be modulated by the magnetic interactions between the magnetised particles.

4.5.2. Electric motors components

Hard-magnetic composites can be applied in electric machines due to their favourable magnetic and mechanical properties, as well as the possibility of tailoring their physical properties. Magnetic composites in electric motors can be used to reduce the volume of magnetic circuits in electric machines. They can appropriately be shaped improving the efficiency of electric units working at a frequency above 300Hz [154]. The properties of magnetic composites allow the constructors to design new structures of their magnetic circuits, which are better adapted to the customer requirements and allow for reducing the size and weight of electric motors.

5. Conclusions and future perspectives

In this article, we present an overview of the current state of the art of hard-magnetic soft composites (hMAPs), providing the main fundamentals covering all the relevant perspectives. The synthesis methods for hMAPs are presented along with the key experimental characterisation techniques. Then, various constitutive modelling approaches across the length scales to model these fast-growing composites are explained. Afterwards, a wide range of potential applications for hMAPs are described in details. In this section, we finally conduct a critical analysis from each of the perspectives tackled and provide future avenues and unmet questions in the field. Note that most of the following discussion relates to the authors' perspective for the hMAPs field.

Regarding the synthesis of hMAPs, the traditional manufacturing methods, mainly based on the injection moulding, have limited scopes for further advancements. In the last few years, the emergence of novel 3D printing techniques has allowed for breaking the roadblocks impeding the advancement in the area. This has relevantly impacted the field leading to a completely new world of functional devices of different size-scales, with a huge innovation on the soft robotics and biomedical engineering areas. However, we still need of further research to understand not only the behaviour of the final manufactured hMAPs, but also the multi-physical processes occurring during the manufacturing stage. This will optimise the magneto-mechanical responses of the multifunctional composites and will potentially provide new routes to reconfigure the programmed structural transitions in a fast and efficient manner.

In addition, further experimental characterisation campaigns are also needed to understand the influence of the magnetic interactions on the mechanical response of the hMAPs. More precisely, there are needs for experiments revealing the evolution of the magnetic response during the material deformation in different modes (i.e., shear, uniaxial compression and tension, biaxial). The influence of viscous mechanisms on the magneto-mechanical performance of these composites is also a matter of current discussion, as well as the influence of the nature of different polymeric matrices, magnetic particles and their interactions along the interphase. A major portion of potential applications for hMAPs are related to active devices e.g., soft robots for high precision drug delivery, stretchable sensors etc, that might have direct contacts with human. Hence, both matrix materials and fillers must be biocompatible so that they will not irritate human body. There are few biocompatible hydrogels that can be easily used as the matrix materials. However, other than few silicones polymers, biocompatible elastomeric matrices are very limited. Hence, more chemistry routes need to be investigated for the manufacturing of biocompatible polymers.

On the modelling part, there is still an open discussion on the conceptualisation of the magneto-mechanical problem, e.g., if the Zeeman effect (effect of the external magnetic field on a magnetised hMAP) is the only major player or if, contrarily, dipole-dipole interactions between the hard particles need to be accounted for. In addition, multiscale models linking the microstructural features to the macroscopic response (i.e., homogenisation approaches) would help at understanding better the different deformation mechanisms involved. However, these multiscale computational techniques are computationally expensive that need to be efficient in time applying various reduced order modelling methods. Further modelling research may address the manufacturing process to identify the key parameters determining the resulting materials. These models would help at optimising the programmed responses of the components and would reduce expenses and timing costs.

Relying on the aforementioned manufacturing, characterization and modelling techniques, hMAPs enable a wide range of new applications that were considered unreachable in the past. The basic applications presented here can be integrated into more sophisticated systems, leading to the design and optimization of a new generation of smart devices, such as miniaturized robotics, complex morphing nano-micromechanisms, innovative biomedical devices, and outer space structures. Moreover, till today, most of the potential applications of hMAPs discussed in the literature are mainly actuators for soft robotics. Hence, multiple active mechanisms, e.g. sensation, actuation, and energy harvesting should be integrated in a system made of hMAP. For such an integration, more works need to be done in the near future. Finally, the design process of hMAPs will be probably addressed by the combination of modelling and 3D printing techniques helped by artificial intelligence tools (i.e., machine learning applied to computational predictive tools). In this regard, the advance in modelling approaches will allow for better predictive tools that can be used to guide the manufacturing process. Thus, more complex and sophisticated applications would be accessible. In addition, further study on procedures to improve the biocompatibility of the hMAP filler particles will definitely open a ”big door” for in vivo multifunctional devices.

Acknowledgement

The authors acknowledge support from the European Research Council (ERC) under the European Union’s Horizon 2020 research and innovation programme (grant agreement No. 947723, project: 4D-BIOMAP). DGG acknowledges support from the Talent Attraction grant (CM 2018 - 2018-T2/IND-9992) from the Comunidad de Madrid. MH acknowledges the funding through an EPSRC Impact Acceleration Award (EP/R511614/1).

References

[1] Tajeddini, V., Muliana, A., 2017. Deformations of flexible and foldable electro-active composite structures. Composite Structures, 160:280-291.

[2] dos Santos, C.R., Pacheco, D.R.Q., Taha, H.E., Zakaria, M.Y., 2021. Nonlinear modeling of electro-aeroelastic dynamics of composite beams with piezoelectric coupling. Composite Structures, 255:112968.

[3] Ren, Z., Hu, W., Dong, X., Sitti, M., 2019. Multi-functional soft-bodied jellyfish-like swimming. Nature Communications, 10:2703.

[4] Kim, Y., Yuk, H., Zhao, R., Chester, S. A., Zhao., X., 2018. Printing ferromagnetic domains for untethered fast-transforming soft materials. Nature, 558 (7709): 274-27.

[5] Garcia-Gonzalez, D., Moreno M.A., Valencia L, Arias A, Velasco D., 2021. Influence of Elastomeric Matrix and Particle Volume Fraction on the Mechanical Response of Magneto-Active Polymers, Composites Part B: Engineering, 215: 108796.

[6] Zare, M., Prabhakaran, M.P., Parvin, N., Ramakrishna, S., 2019. Thermally-induced two-way shape memory polymers: Mechanisms, structures, and applications, Chemical Engineering Journal, 374:706-720.

[7] Jiao, P., Chen, T., Xie, Y., 2021. Self-adaptive mechanical metamaterials (SMM) using shape memory polymers for programmable postbuckling under thermal excitations. Composite Structures, 256:113053.

[8] Yu, K., Xin, A., Wang, Q., 2019. Mechanics of light-activated self-healing polymer networks. Journal of the Mechanics and Physics of Solids, 124:643-662.

[9] Zhang, C., Li, J., Yang, C., Gong, S., Jiang, H., Sun, M., Qian, C., 2020. A pH-sensitive coordination polymer network-based nanoplatform for magnetic resonance imaging-guided cancer chemo-photothermal synergistic therapy. Nanomedicine: Nanotechnology, Biology and Medicine, 23:102071.

[10] Kim, Y., Parada, G.A., Liu, S., Zhao, X., 2019. Ferromagnetic soft continuum robots. Science Robotics, 4(33):eaax7329.

[11] Hu, W., Lum, G., Mastrangeli, M., Sitti M., 2018. Small-scale soft-bodied robot with multimodal locomotion. Nature, 554:81–85.

[12] Lu, H., Zhang, M., Yang, Y. et al. 2018. A bioinspired multilegged soft millirobot that functions in both dry and wet conditions. Nature Communications, 9:3944.

[13] Penumakala, P.K., Santo, J., Thomas, A., 2020. A critical review on the fused deposition modeling of thermoplastic polymer composites. Composites Part B: Engineering, 201:108336.

[14] Garcia-Gonzalez, D., Landis, C.M., 2020. Magneto-diffusion-viscohyperelasticity for magneto-active hydrogels: rate dependences across time scales. Journal of the Mechanics and Physics of Solids, 139:103934.

[15] Kankanala, S.V., Triantafyllidis, N., 2004. On finitely strained magnetorheological elastomers. Journal of the Mechanics and Physics of Solids, 52:2869-2908.

[16] Garcia-Gonzalez, D., Hossain, M., 2020. A microstructural-based approach to model magneto-viscoelastic materials at finite strains. International Journal of Solids and Structures, 208-209:119-132.

[17] Zhao, R., Kim, Y., Chester, A. S., Sharma, P., Zhao, X., 2019. Mechanics of hard-magnetic soft materials. Journal of the Mechanics and Physics of Solids, 124:244-263.

[18] Lum, G. Z., Ye, Z., Dong, X., Marvi, H., Erin, O., Hu, W., Sitti, M., 2016. Shape-programmable magnetic soft matter. Proceedings of the National Academy of Sciences, 113(41):E6007-E6015.

[19] Zhao, X., Kim, J., Cezar, C.A., Huebsch, N., Lee, K., Bouhadir, K., Mooney, D.J., 2011. Active scaffolds for on-demand drug and cell delivery. Proceedings of the National Academy of Sciences, 108(1):67-72.

[20] Liu, J.A.-C., Gillen, J.H., Mishra, S.R., Evans, B.A., Tracy, J.B., 2019. Photothermally and magnetically controlled reconfiguration of polymer composites for soft robotics. Science Advances 5(8):eaaw2897.

[21] Garcia-Gonzalez, D., Hossain, M., 2021. Microstructural modelling of hard-magnetic soft materials: Dipole-dipole interactions versus Zeeman effect, Under Review.

[22] Wei, H., Zhang, Q., Yao, Y., Liu, L., Liu, Y., Leng, L. 2017. Direct-Write Fabrication of 4D Active Shape-Changing Structures Based on a Shape Memory Polymer and Its Nanocomposite, ACS Applied Materials & Interfaces, 9:876-883.

[23] Breger, J. C., Yoon, C. K., Xiao, R. Kwag H. R., Wang M. O., Fisher J. P., Nguyen T. D. 2015. Self-folding thermo-magnetically responsive soft microgrippers, ACS applied materials & interfaces, 7 (5):3398-3405

[24] Ligon, S.C., Liska, R., Stampfl, J., Gurr, M., Huelhaupt, R., 2017. Polymers for 3D printing and customized additive manufacturing. Chemical Reviews, 10212-10290,117:2017.

[25] Wang, L., Kim, Y., Guo, G.F., Zhao, X., 2020. Hard-magnetic elastica. Journal of the Mechanics and Physics of Solids, 142:104045.

[26] Rafiee, M., Farahani, R.D., Therriault, D., 2020. Multi-material 3D and 4D printing: A survey. Advanced Science, 7:1902307.

[27] T. Billiet, T., Vandenhaute, M., Schelfhout, J., Van Vlierberghe, S., Dubruel, P. 2012. A review of trends and limitations in hydrogel-rapid prototyping for tissue engineering, Biomaterials, 33:6020-6041.

[28] Ning, F. D., Cong, W. L., Qiu, J. J., Wang, J. H., Wang, S. R. 2015. Additive manufacturing of carbon fiber reinforced thermoplastic composites using fused deposition modeling, Composites, Part B, 80:369-378.

[29] Norman, J., Madurawe, R. D., Moore, C. M., Khan, M. A., Khairuzzaman, A. 2017. A new chapter in pharmaceutical manufacturing: 3D-printed drug products, Adv. Drug Delivery Rev., 108, 39-50.

[30] Li, J., Wu, C., Chu, P.K., Gelinsky, M., 2020. 3D printing of hydrogels: Rational design strategies and emerging biomedical applications. Materials Science and Engineering R 140:100543.

[31] Tumbleston, J.R., Shirvanyants, D., Ermoshkin, N., Janusziewicz, R., Johnson, A.R., Kelly, D., Chen, K., Pinschmidt, R., Rolland, J.P., Ermoshkin, A., Samulski, E.T., DeSimone, J.M., 2015. Continuous liquid interface production of 3D objects. Science, 347(6228).

[32] Hossain, M., Navaratne, R., Peric, D., 2020. 3D printed elastomeric polyurethane: Viscoelastic experimental characterizations and constitutive modelling with nonlinear viscosity functions. International Journal of Non-Linear Mechanics, 126:103546.

[33] Domingo-Roca, R., Jackson, J C., Winmill, J F C., 2018. 3D-printing polymer-based permanent magnets. Materials and Design, 153:120-128.

[34] Tareq, M S., Rahman, T., Hossain, M., Dorrington, P., 2021. Additive manufacturing and the COVID-19 challenges: An in-depth study. Journal of Manufacturing Systems, In Press.

[35] Bastola, A K., Hossain, M., 2020. A review on magneto-mechanical characterizations of magnetorheological elastomers. Composites Part B: Engineering, 200:108348.

[36] Bastola, A. K., Paudel, M., Li, L. 2018. Development of hybrid magnetorheological elastomers by 3D printing, Polymer, 149:213-228

[37] Bastola, A K., Hossain, M., 2021. Enhanced performance of core-shell hybrid magnetorheological elastomer with nanofillers, Materials Letters, 129944

[38] Mukherjee, D., Rambausek, M., Danas, K., 2021. An explicit dissipative model for isotropic hard magnetorheological elastomers. Journal of the Mechanics and Physics of Solids, 151:104361.

[39] Hossain, M., Saxena, P., Steinmann, P., 2015. Modelling the mechanical aspects of the curing process of magneto-sensitive elastomeric materials. International Journal of Solids and Structures, 58: 257-269

[40] Hossain, M., Chatzigeorgiou, G., Meraghni, F., Steinmann, P., 2015. A multi-scale approach to model the curing process in magneto-sensitive polymeric materials. International Journal of Solids and Structures, 69-70:34-44

[41] Haldar, K., Kiefer, B., Menzel, A. 2016. Finite element simulation of rate-dependent magneto-active polymer response, Smart Materials and Structures, 25(10):104003

[42] Garcia-Gonzalez, D., 2019. Magneto-visco-hyperelasticity for hard-magnetic soft materials: theory and numerical applications. Smart Materials and Structures, 28:085020

[43] Dorfmann, A, Ogden, R.W., 2004. Nonlinear magnetoelastic deformations of elastomers. Acta Mechanica, 167(1-2):13-28.

[44] Mehnert, M., Hossain, M., Steinmann, P. 2017. Towards a thermo-magneto-mechanical coupling framework for magneto-rheological elastomers. International Journal of Solids and Structures, 128:117-132.

[45] A. Dorfmann, R.W. Ogden, 2005. Some problems in nonlinear magnetoelasticity. The Journal of Applied Mathematics and Physics 56 (4): 718–745.

[46] Danas, K., Kankanala, S. V., Triantafyllidis, N., 2012. Experiments and modelling of iron-particled-filled magnetorheological elastomers. Journal of the Mechanics and Physics of Solids 60(1):120-138.

[47] Coleman, B.D., Gurtin, M.E., 1967. Thermodynamics with internal state variables. Journal of Chemical Physics, 47:597-613.

[48] Maugin, G.A., 1988. Continuum Mechanics of Electromagnetic Solids. North Holland, Amsterdam.

[49] Kadapa, C., Hossain, M., 2020. A linearised consistent mixed displacement-pressure formulation for hyperelasticity. Mechanics of Advanced Materials and Structures, In Press.

[50] de Souza Neto, E.D., Peric, D., Owen, D.R.J., 2008. Computational methods for plasticity: theory and applications. Wiley.

[51] Hong, W., Zhao, X., Zhou, J., Suo, Z., 2008. A theory of coupled diffusion and large deformation in polymeric gels. Journal of the Mechanics and Physics of Solids 56(5):1779-1793.

[52] Chen, W., and Wang, L., 2020. Theoretical Modeling and Exact Solution for Extreme Bending Deformation of Hard-Magnetic Soft Beams. ASME Journal of Applied Mechanics, 87(4):041002.

[53] Chen, W., Yan, Z., Wang, L., 2020. On mechanics of functionally graded hard-magnetic soft beams. International Journal of Engineering Science, 157:103391.

[54] Dzhezherya, Y.I., Kalita, V.M., Cherepov, S.V., Skirta, Y.B., Berezhnaya, L.V., Levchenko, G.G., 2019. Anomalous behavior of bending deformation induced by a magnetic field in a system of ferromagnetic stripes located on an elastomer. Smart Materials and Structures 28:125013.

[55] Gong, X., Tan, K., Deng, Q., Shen, S., 2020. Athermal Shape Memory Effect in Magnetoactive Elastomers. ACS Applied Materials and Interfaces, 12(14):16930-16936.

[56] Ma, C., Wu, S., Ze, Q., Kuang, X., Zhang, R., Qi, H.J., Zhao, R., 2020. Magnetic Multimaterial Printing for Multimodal Shape Transformation with Tunable Properties and Shiftable Mechanical Behaviors, ACS Applied Materials and Interfaces Article, 13(11):12639–12648.

[57] Chen, W., Wang, L., Yan, Z., Luo, B., 2021. Three-dimensional large-deformation model of hard-magnetic soft beams. Composite Structures, 266, 113822.

[58] Ye, H., Li, Y., Zhang, T., 2020. Magttice: A Lattice Model for Hard-Magnetic Soft Materials. Soft Matter, 17, 3560-3568.

[59] Ivaneyko, D., Toshchevikov, V., Saphiannikova, M., Heinrich, G., 2012. Effects of particle distribution on mechanical properties of magneto-sensitive elastomers in a homogeneous magnetic field. Condensed Matter Physics 15, 33601.

[60] Zhang, R., Wu, S., Qiji, Z., Zhao, Z., 2020. Micromechanics Study on Actuation Efficiency of Hard-Magnetic Soft Active Materials. Journal of Applied Mechanics, 87:091008.

[61] Nadzharyan, T.A., Stolbov, O.V., Raikher, Y.L, Kramarenko, E.Y., 2019. Field-induced surface deformation of magnetoactive elastomers with anisometric fillers: a single-particle model. Soft Matter, 15:9507-9519.

[62] Kalina, K.A., Brummund, J., Metsch, M., Kästner, M., Borin, D.Y.,Linke, J.M., Odenbach, S., 2017. Modeling of magnetic hystereses in soft MREs filled with NdFeB particles. Smart Mater. Struct. 26:105019.

[63] Zabihyan, R., Mergheim, J., Javili, A., Steinmann, P., 2018. Aspects of computational homogenization in magneto-mechanics: Boundary conditions, RVE size and microstructure composition. International Journal of Solids and Structures, 130-131:105-121.

[64] Zabihyan, R., Mergheim, J., Pelteret, J.P., Brands, B., Steinmann, P., 2020. FE2 simulations of magnetorheological elastomers: influence of microscopic boundary conditions, microstructures and free space on the macroscopic responses of MREs. International Journal of Solids and Structures, 193-194:338-356.

[65] Mukherjee, D., Bodelot, L., Danas, K., 2020. Microstructurally-guided explicit continuum models for isotropic magnetorheological elastomers with iron particles. International Journal of Non-Linear Mechanics, 120:103380.

[66] Sanchez, P.A., Stolbov, O.V., Kantorovich, S.S., Raikher, Y.L., 2019. Modeling the magnetostriction effect in elastomers with magnetically soft and hard particles. Soft Matter, 15:7145.

[67] Becker, T.I., Stolbov, O.V., Borin, D.Y., Zimmermann, K., Raikher, Y.L., 2020. Basic magnetic properties of magnetoactive elastomers of mixed content. Smart Mater. Struct., 29:075034.

[68] Wu, S., Hu, W., Ze, Q., Sitti,M., Zhao,R., 2020. Multifunctional magnetic soft composites: a review. Multifunctional Materials, 3:042003.

[69] Hines, L., Petersen, K., Lum, G. Z., Sitti, M., 2017. Soft Actuators for Small-Scale Robotics. Advanced Materials, 29:1603483.

[70] Boyraz, P., Runge, G., Raatz, A., (2018). An Overview of Novel Actuators for Soft Robotics. Actuators, 7:48.

[71] Erb, R.M., Martin, J.J., Soheilian, R., Pan, C. and Barber, J.R., 2016. Actuating Soft Matter with Magnetic Torque. Advanced Functional Materials, 26:3859-3880.

[72] Do, T. N., Phan, H., Nguyen, T.-Q., Visell, Y., 2018. Miniature Soft Electromagnetic Actuators for Robotic Applications. Advanced Functional Materials, 28:1800244.

[73] Ausanio, G., Iannotti, V., Hison, C., Lanotte, L., D'Agostino, A., Germano, R., 2004. Novel elastic magnets as actuators core. Applied Electromagnetics and Mechanics, 19:395-398.

[74] von Lockette, P., Lofland, S.E., Biggs, J., Roche, J., Mineroff J., Babcock, M., 2011. Investigating new symmetry classes in magnetorheological elastomers: cantilever bending behavior. Smart Materials and Structures, 20:105022.

[75] Koo, J.H., Dawson, A., Jung, H.J., 2012. Characterization of actuation properties of magnetorheological elastomers with embedded hard magnetic particles. Journal of Intelligent Material Systems and Structures, 23(9):1049–1054.

[76] Lee, M., Park, T., Kim, C., Park, S.M. 2020. Characterization of a magneto-active membrane actuator comprising hard magnetic particles with varying crosslinking degrees. Materials and Design, 195:108921,

[77] Song, H., Lee, H., Lee, J., Choe, J.K., Lee, S., Yi, J.Y., Park, S., Yoo, J.W., Kwon, M.S., Kim, J., 2020. Reprogrammable Ferromagnetic Domains for Reconfigurable Soft Magnetic Actuators. Nano Letters, 20:5185–5192

[78] Ze, Q., Kuang, X., Wu, S., Wong, J., Montgomery, S. M., Zhang, R., Kovitz, J. M., Yang, F., Qi, H. J., Zhao, R., 2019. Magnetic Shape Memory Polymers with Integrated Multifunctional Shape Manipulation. Advanced Materials, 32:1906657.

[79] Lei, Y., Sheng, Z., Zhang, J. et al. Building Magnetoresponsive Composite Elastomers for Bionic Locomotion Applications. J Bionic Eng 17, 405–420 (2020).

[80] Diller, E. and Sitti, M., 2014. Three-Dimensional Programmable Assembly by Untethered Magnetic Robotic Micro-Grippers. Advanced Functional Materials 24: 4397-4404.

[81] Chung, S.E., Dong X., Sitti, M., 2015. Three-dimensional heterogeneous assembly of coded microgels using an untethered mobile microgripper. Lab Chip, 15:1667-1676.

[82] Zhang,J., Onaizah, O., Middleton, K., You, L., Diller, E., 2017. Reliable Grasping of Three-Dimensional Untethered Mobile Magnetic Microgripper for Autonomous Pick-and-Place. IEEE Robotics and Automation Letters 2:835-840.

[83] Shintake, J., Cacucciolo, V., Floreano, D., Shea, H., 2018. Soft Robotic Grippers, Advanced Materials, 30:1707035.

[84] Wallin, T.J., Pikul, J., Shepherd, R.F., 2018. 3D printing of soft robotic systems. Nature Reviews Materials 3:84–100.

[85] Xu, T., Zhang, J., Salehizadeh, M., Onaizah O., Diller, E., 2019. Millimeter-scale flexible robots with programmable three-dimensional magnetization and motions. Science Robotics, 4(29):eaav4494.

[86] Xu, C., Yang, Z., Lum, G. Z., 2021. Small-Scale Magnetic Actuators with Optimal Six Degrees-of-Freedom. Advanced Materials, 2100170.

[87] Zhang J., Diller, E., 2016. Tetherless mobile micrograsping using a magnetic elastic composite material. Smart Materials and Structures, 25:11LT03.

[88] Zhang, J., Salehizadeh, M., Diller, E.,2018. Parallel Pick and Place Using Two Independent Untethered Mobile Magnetic Microgrippers. IEEE International Conference on Robotics and Automation (ICRA), 2018:123-128,

[89] Chung, S.E., Dong, X., Sitti, M., 2015. Three-dimensional heterogeneous assembly of coded microgels using an untethered mobile microgripper, Lab Chip, 2015,15, 1667-1676

[90] Dong, X., Sitti, M., 2017. Planning spin-walking locomotion for automatic grasping of microobjects by an untethered magnetic microgripper. IEEE International Conference on Robotics and Automation (ICRA), 2017:6612-6618.

[91] Zhang, Z., Chen, D., Wu, H., Bao, Y., Chai, G., 2016. Non-contact magnetic driving bioinspired Venus flytrap robot based on bistable anti-symmetric CFRP structure. Composite Structures, 135, 17-22.

[92] Zhang, Z., Li, X., Yu, X., Chai, H., Li, Y., Wu, H., Jiang, S., 2019. Magnetic actuation bionic robotic gripper with bistable morphing structure. Composite Structures, 229, 111422.

[93] Mitsumata, T., Horikoshi, Y., Takimoto, J., 2007. Flexible Fluid Pump Using Magnetic Composite Gels, e-Polymers, 7(1):147.

[94] Mohd Said, M., Yunas, J., Bais, B., Hamzah, A. A., Yeop Majlis, B., 2017. The Design, Fabrication, and Testing of an Electromagnetic Micropump with a Matrix-Patterned Magnetic Polymer Composite Actuator Membrane. Micromachines, 9(1):13.

[95] Becker, T.I., Zimmermann, K., Borin, D.Y., Stepanov, G.V., Storozhenko, P.A., 2018. Dynamic response of a sensor element made of magnetic hybrid elastomer with controllable properties. Journal of Magnetism and Magnetic Materials 449, 77-82.

[96] Alfadhel, A., Kosel, J., 2015. Magnetic nanocomposite cilia tactile sensor. Advanced Materials, 27:7888-7892.

[97] Ge, J., Wang, X., Drack, M., Volkov, O., Liang, M., Cañón-Bermúdez, G.S. Illing, R, Wang, C., Zhou, S., Fassbender, J., Kaltenbrunner M., Makarov, D., 2019. A bimodal soft electronic skin for tactile and touchless interaction in real time. Nature Communications 10:4405.

[98] Almansouri, A. S., Alsharif, N. A., Khan, M. A., Swanepoel, L., Kaidarova, A., Salama, K. N., Kosel, J., 2019. An imperceptible magnetic skin. Advanced Materials Technologies, 4:1900493.

[99] Panina, L., Ipatov, M., Gonzalez, J., Zhukova, V., Zhukov, A., 2011. Tuneable composites containing magnetic microwires, metal, ceramic and polymeric composites for Various Uses. Dr. John Cuppoletti (Ed.)

[100] Peng, H.X., Qin, F.X.,. Phan, M.H, Tang, J., Panina, L.V., Ipatov, M., Zhukova, V., Zhukov, A., Gonzalez, J., 2009. Co-based magnetic microwire and field-tunable multifunctional macro-composites. Journal of Non-Crystalline Solids, 355(24–27):1380-1386,

[101] Ng, C. S. X., Tan, M. W. M., Xu, C., Yang, Z., Lee, P. S., Lum, G. Z., 2021. Locomotion of Miniature Soft Robots. Advanced Materials 33, 2003558.

[102] Wang, X., Mao, G., Ge, J. et al. Untethered and ultrafast soft-bodied robots. Communications Materials 1:67.

[103] Kim, J.G., Park, J.E., Won, S., Jeon, J., Wie, J.J., 2019. Contactless Manipulation of Soft Robots. Materials, 12:3065.

[104] Eshaghi, M., Ghasemi, M., Khorshidi, K., 2021. Design, manufacturing and applications of small-scale magnetic soft robots. Extreme Mechanics Letters, 44:101268.

[105] Wang, L., Zheng, D., Harker, P., Patel, A.B., Guo, C.F, Zhao, X., 2021. Evolutionary design of magnetic soft continuum robots. Proceedings of the National Academy of Sciences, 118(21):e2021922118.

[106] Sitti, M., 2018. Miniature soft robots — road to the clinic. Nature Reviews Materials 3:74–75.

[107] Floyd, S., Diller, E., Pawashe, C., Sitti, M., 2011. Control methodologies for a heterogeneous group of untethered magnetic micro-robots. The International Journal of Robotics Research, 30(13):1553-1565.

[108] Diller, E., Pawashe, C., Floyd, S., Sitti, M., 2011. Assembly and disassembly of magnetic mobile micro-robots towards deterministic 2-D reconfigurable micro-systems. The International Journal of Robotics Research, 30(14):1667-1680.

[109] Alapan, Y., Karacakol, A.C., Guzelhan, S.N., Isik I., Sitti, M., 2020. Reprogrammable shape morphing of magnetic soft machines. Science Advances, 6(38):eabc6414.

[110] Shinoda, H., Azukizawa, S., Maeda, K., Tsumori, F., 2019. Bio-mimic motion of 3D-printed gel structures dispersed with magnetic particles. Journal of The Electrochemical Society, 166:B3235.

[111] Wu, S., Ze, Q., Zhang, R., Hu, N., Cheng, Y., Yang, F., Zhao, R., 2019. Symmetry-breaking actuation mechanism for soft robotics and active metamaterials. ACS Applied Materials and Interfaces, 11(44):41649-41658.

[112] Wu, S., Hamel, C.M., Ze, Q., Yang, F., Qi, H.J. and Zhao, R., 2020. Evolutionary algorithm-guided voxel-encoding printing of functional hard-magnetic soft active materials. Advanced Intelligent Systems, 2:2000060.

[113] Tasoglu, S., Diller, E., Guven, S. et al., 2014. Untethered micro-robotic coding of three-dimensional material composition. Nature Communications, 5:3124.

[114] Bi, C., Guix, M., Johnson, B. V., Jing, W., Cappelleri, D. J., 2018. Design of microscale magnetic tumbling robots for locomotion in multiple environments and complex terrains. Micromachines, 9(2), 68.

[115] Jing, W., Pagano, N., Cappelleri, D.J., 2013. A novel micro-scale magnetic tumbling microrobot. Journal of Micro-Bio Robotics, 8:1–12.

[116] Zhang, J., Guo, Y., Hu, W., Soon, R. H., Davidson, Z. S., Sitti, M., 2021. Liquid Crystal Elastomer-Based Magnetic Composite Films for Reconfigurable Shape-Morphing Soft Miniature Machines. Advanced Materials, 33:2006191.

[117] Salehizadeh, M., Diller, E., 2017. Two-agent formation control of magnetic microrobots in two dimensions. Journal of Micro-Bio Robotics, 12:9–19.

[118] Salehizadeh M, Diller E., 2020. Three-dimensional independent control of multiple magnetic microrobots via inter-agent forces. The International Journal of Robotics Research. 39(12):1377-1396.

[119] Xu, T., Yu, J., Yan, X., Choi, H., Zhang, L, 2015. Magnetic Actuation Based Motion Control for Microrobots: An Overview. Micromachines, 6(9):1346-1364.

[120] Pawashe, C., Floyd, S., Sitti, M., 2009. Multiple magnetic microrobot control using electrostatic anchoring. Applied Physics Letters 94:164108.

[121] Zhang, J., Diller, E., 2018. Untethered miniature soft robots: modeling and design of a millimeter-scale swimming magnetic sheet. Soft Robotics, 5-6:761-776

[122] Qiu, T., Lee, T.C., Mark, A., Morozov, K.I., Münster, R., Mierka, O., Turek, S., Leshansky, A. M., Fischer, P., 2014. Swimming by reciprocal motion at low Reynolds number. Nature Communications 5:5119.

[123] Manamanchaiyaporn, L., Xu, T., Wu, X., 2020. Magnetic Soft Robot With the Triangular Head–Tail Morphology Inspired By Lateral Undulation. IEEE/ASME Transactions on Mechatronics, 25(6):2688-2699.

[124] Diller, E., Zhuang, J., Lum, G.Z., Edwards, M. R., Sitti, M., 2014. Continuously distributed magnetization profile for millimeter-scale elastomeric undulatory swimming. Applied Physics Letters 104:174101.

[125] Ye, Z., Régnier, S., Sitti, M., 2014. Rotating magnetic miniature swimming robots with multiple flexible flagella. IEEE Transactions on Robotics, 30(1):3-13.

[126] Wang, T., Ren, Z., Hu, W., Li, M., Sitti, M., 2021. Effect of body stiffness distribution on larval fish–like efficient undulatory swimming. Science Advances 7(19):eabf7364.

[127] Zhang, J., Jain, P., Diller, E., 2016. Independent control of two millimeter-scale soft-bodied magnetic robotic swimmers. IEEE International Conference on Robotics and Automation (ICRA), 2016:1933-1938.

[128] Wu, Z., Troll, J., Jeong, H.H., Wei, Q., Stang, M., Ziemssem, F., Wang, Z., Dong, M., Schnichels, S., Qiu, T., Fischer P., 2018. A swarm of slippery micropropellers penetrates the vitreous body of the eye Science Advances, 4(11):eaat4388.

[129] Zhang, J., Diller, E., 2015. Millimeter-scale magnetic swimmers using elastomeric undulations IEEE/RSJ International Conference on Intelligent Robots and Systems (IROS), 2015:1706-1711,

[130] Gu, H., Boehler, Q., Cui, H. et al., 2020. Magnetic cilia carpets with programmable metachronal waves. Nature Communications 11:2637.

[131] Timonen, J.V.I., Johans, C., Kontturi, K., Walther, A., Ikkala, O., Ras, R.H.A., 2010. A facile template-free approach to magnetodriven, multifunctional artificial cilia. ACS Applied Materials and Interfaces, 2(8):2226–2230.

[132] Dong, X., Lum, G.Z., Hu, W., Zhang, R., Ren, Z., Onck, P.R., Sitti, M., 2020. Bioinspired cilia arrays with programmable nonreciprocal motion and metachronal coordination. Science Advances, 6(45):eabc9323.

[133] Wu, Z., Chen, Y., Mukasa, D., Pak, S., Gao, W., 2020. Medical micro/nanorobots in complex media. Chemical Society Reviews, 49:8088-8112.

[134] Hwang, J., Kim, Jy., Choi, H., 2020. A review of magnetic actuation systems and magnetically actuated guidewire- and catheter-based microrobots for vascular interventions. Intelligent Service Robotics 13:1–14.

[135] Chautems, C., Zeydan, B., Charreyron, S., Chatzipirpiridis, G., Pané, S., Nelson, B.J., 2017. Magnetically powered microrobots: a medical revolution underway? European Journal of Cardio-Thoracic Surgery, 51(3):405-407.

[136] Ebrahimi, N., Bi, C., Cappelleri, D. J., Ciuti, G., Conn, A. T., Faivre, D., Habibi, N., Hošovský, A., Iacovacci, V., Khalil, I. S. M., Magdanz, V., Misra, S., Pawashe, C., Rashidifar, R., Soto-Rodriguez, P. E. D., Fekete, Z., Jafari, A., 2021. Magnetic Actuation Methods in Bio/Soft Robotics. Advanced Functional Materials, 31:2005137.

[137] Sliker, L., Ciuti, G., Rentschler, M., Menciassi A., 2015. Magnetically driven medical devices: a review. Expert Review of Medical Devices, 12(6):737-752

[138] Iacovacci, V., Lucarini, G., Ricotti, L. et al. 2015. Untethered magnetic millirobot for targeted drug delivery. Biomed Microdevices, 17:63

[139] Lucarini, G., Iacovacci, V., Gouveia, P.J., Ricotti, L., Menciassi, A., 2018. Design of a novel magnetic platform for cell manipulation. Journal of Micromechanics and Microengineering, 28:025009.

[140] Lee D. W., Kim S. H., Kozlov M. E., Lepro X., Baughman R. H., Kim S. J., 2018. Magnetic torsional actuation of carbon nanotube yarn artificial muscle. RSC Advances, 8:17421-17425.

[141] Nguyen, V.Q., Ahmed, A.S., Ramanujan, R.V. 2012. Morphing soft magnetic composites. Advanced Materials, 24(30):4041-54.

[142] Nguyen, V.Q. and Ramanujan, R.V. 2010. Novel Coiling Behavior in Magnet-Polymer Composites. Macromolecular Chemistry and Physics, 211:618-626.

[143] Zhang, J., Ren, Z., Hu, W., Soon, R.H., Yasa, I.C., Liu, Z., Sitti, M., 2021. Voxelated three-dimensional miniature magnetic soft machines via multimaterial heterogeneous assembly. Science Robotics, 28:6(53)eabf0112.

[144] Weber, N., Hertkorn, D., Zappe, H., Seifert, A., 2012. Polymer/silicon hard magnetic micromirrors. Journal of Microelectromechanical Systems, 21(5):1098-1106.

[145] Novelino, L.S., Ze, Q., Wu, S., Paulino, G.H., Zhao, R., 2020. Untethered control of functional origami microrobots with distributed actuation. Proceedings of the National Academy of Sciences, 117(39):24096-24101.

[146] Yu, K., Fang, N. X., Huang, G., Wang, Q., 2018. Magnetoactive acoustic metamaterials, Advanced Materials 30:1706348.

[147] Montgomery, S. M., Wu, S., Kuang, X., Armstrong, C. D., Zemelka, C., Ze, Q., Zhang, R., Zhao, R., Qi, H. J., 2021. Magneto-mechanical metamaterials with widely tunable mechanical properties and acoustic bandgaps. Advanced Functional Materials 31, 2005319.

[148] Lee, K., Yu, K., Al B., Hasan B., Xin, A., Feng, Z. 2020. Sharkskin-inspired magnetoactive reconfigurable acoustic metamaterials. Research 2020:1-13.

[149] Chen, T., Pauly, M., Reis, P.M., 2021. A reprogrammable mechanical metamaterial with stable memory. Nature 589:386–390.

[150] Keller, M.W., Crall, M.D., 2018. Self-healing composite materials. Comprehensive Composite Materials II (Chapter 6), Elsevier, 431-453.

[151] Hohlbein, N., Shaaban, A., Schmidt, A.M., 2015. Remote-controlled activation of self-healing behavior in magneto-responsive ionomeric composites. Polymer, 69:301-309,

[152] Abramchuk, S., Kramarenko, E., Grishin, D., Stepanov, G., Nikitin, L.V., Filipcsei, G., Khokhlov, A.R. and Zrínyi, M., 2007. Novel highly elastic magnetic materials for dampers and seals: part II. Material behavior in a magnetic field. Polymers for Advanced Technologies, 18:513-518.

[153] Stepanov, G.V., Borin, D.Y., Kramarenko, E.Y., V. V. Bogdanov, D. A. Semerenko, P. A. Storozhenko, 2014. Magnetoactive elastomer based on magnetically hard filler: Synthesis and study of viscoelastic and damping properties. Polymer Science, Series A, 56:603–613.

[154] Najgebauer M., Szczyglowski J., Slusarek B., Przybylski M., Kaplon A., Rolek J., 2018. Magnetic composites in electric motors. Analysis and Simulation of Electrical and Computer Systems. Lecture Notes in Electrical Engineering, 452, Springer.

[155] Stepanov, G.V., Chertovich, A.V., Kramarenko, E. Y. 2012. Magnetorheological and deformation properties of magnetically controlled elastomers with hard magnetic filler, Journal of Magnetism and Magnetic Materials 324: 3448-3451

[156] Antonel, P. S., Jorge, G., Perez, O. E., Butera, A., Leyva, A. G., Negri, R. M., 2011. Magnetic and elastic properties of $CoFe_2O_4$- polydimethylsiloxane magnetically oriented elastomer nanocomposites, Journal of Applied Physics, 110: 043920

[157] Kramarenko, E. Y., Chertovich, A. V., Stepanov, G. V., Semisalova, A. S., Makarova, L. A., Perov, N. S., Khokhlov, A. R., 2015. Magnetic and viscoelastic response of elastomers with hard magnetic filler, Smart Materials and Structures, 24(3):035002

[158] Koo, J. H., Dawson, A., Jung, H J., 2012. Characterization of actuation properties of magnetorheological elastomers with embedded hard magnetic particles, Journal of Intelligent Material Systems and Structures, 23(9):1049-1054

[159] Lee, C. J., Kwon, S. H., Choi, H. J., Chung, K. H., Jung, J. H., 2018. Enhanced magnetorheological performance of carbonyl iron/natural rubber composite elastomer with gamma-ferrite additive, Colloid and Polymer Science, 296:1609-1613

[160] Lee, H., Jang, Y., Choe, J. K., Lee, S., Song, H., Lee, J. P., Lone, N., Kim, J., 2020. 3D-printed programmable tensegrity for soft robotics, Science Robotics, 5:eaay9024.

[161] Hu, K., Sun, J., Guo, Z., Wang, P., Chen, Q., Ma, M., Gu, N. 2015. A Novel Magnetic Hydrogel with Aligned Magnetic Colloidal Assemblies Showing Controllable Enhancement of Magnetothermal Effect in the Presence of Alternating Magnetic Field, Advanced materials, 27:2507-2514.

[162] Sundaram, S., Skouras, M., Kim, D. S., van den Heuvel, L., Matusik, W. 2019. Topology optimization and 3D printing of multimaterial magnetic actuators and displays, Science Advances, 5:eaaw1160

[163] Nagarajan, B., Mertiny, P., Qureshi, A. J. 2020. Magnetically loaded polymer composites using stereolithography-Material processing and characterization, Materials Today Communications, 25:101520

[164] Lantean, S., Barrera, G., Pirri, C. F., Tiberto, P., Sangermano, M., Roppolo, I., Rizza, G., 2019. 3D Printing of Magnetoresponsive Polymeric Materials with Tunable Mechanical and Magnetic Properties by Digital Light Processing, Advanced Materials Technologies, 4: 1900505.

Declaration of interests

☒ The authors declare that they have no known competing financial interests or personal relationships that could have appeared to influence the work reported in this paper.

☐The authors declare the following financial interests/personal relationships which may be considered as potential competing interests: